SUPPLEMENTARY MATERIAL

Benzopyran derivatives from endophytic *Daldinia eschscholzii* JC-15 in *Dendrobium chrysotoxum* and their bioactivities

Ming Hu[#], Xue-Qiong Yang[#], Qing-Yan Zhou, Shu-Quan Li, Bang-Yan Wang, Bao-Hui Ruan, Ya-Bin Yang[*], Zhuo-Xi Zhang, Hao Zhou, Zhong-Tao Ding[*]

Functional Molecules Analysis and Biotransformation Key Laboratory of Universities in Yunnan Province, School of Chemical Science and Technology, Yunnan University.

[#] These authors contributed equally to this paper

Abstract: Five new benzopyran derivatives (**2-6**) and a new natural product (**1**) were isolated from endophytic *Daldinia eschscholzii* in *Dendrobium chrysotoxum* and determined as (R)-2,3-dihydro-2,5-dihydroxy-2-methylchromen-4-one (**1**), (2R, 4S)-2,3-dihydro-2-methyl-benzopyran-4,5-diol (**2**), (R)-3-methoxyl-1-(2,6-dihydroxy phenyl)-butan-1-one (**3**), 7-O-α-D-ribosyl-5-hydroxy-2-methyl-4H-chromen-4-one (**4**), 7-O-α-D-ribosyl-2,3-dihydro-5-hydroxy-2-methyl-chromen-4-one (**5**), daldinium A (**6**). These compounds were evaluated for their antimicrobial activity, anti-acetylcholinesterase, nitric oxide inhibition, anticoagulant, photodynamic antimicrobial activities, and glucose uptake of adipocytes. Some compounds showed photoactive antimicrobial activities and glucose uptake stimulating activities.

Keywords *Daldinia eschscholzii*; benzopyran; *Dendrobium chrysotoxum*; photoactive antimicrobial activity; glucose uptake stimulating activity

1. Experimental

1.1. General experimental procedures

Silica gel (200–300 mesh, Qingdao Marine Chemical Group Co., Qingdao, China), LiChroprep RP-18 (40–63 mm; Merck, Darmstadt, Germany) and Sephadex LH-20 (GE Healthcare Co., Buckinghamshire, UK) were used for column chromatography. 1D and 2D NMR spectra were obtained on a Bruker AVANCE 400, 500, 600 MHz NMR instrument (Bruker, Karlsruhe, Germany). MS spectra were recorded with an Agilent G3250AA (Agilent, Santa Clara, USA) and AutoSpec Premier P776 spectrometer (Waters, Milford, USA). Optical rotations were obtained on a Jasco P-1020 polarimeter.

1.2. Fungus material and fermentation

The endophytic fungus JC-15 was isolated using potato dextrose agar medium (PDA) (peeled and cut potato 200 g/L, glucose 20 g/L, agar 15 g/L) from stems of and *Dendrobium chrysotoxum* was identified as *Daldinia eschscholzii* by ITS gene sequencing. The fungus has been preserved at School of Chemical Science and Technology, Yunnan University, China. The pure strain was stored in 50% glycerol at -80 °C. *Daldinia eschscholzii* was maintained on the PDA medium. Small agar plugs (approximately 5 mm×5 mm) of the fungus were cultured in 0.5 L Erlenmeyer flasks containing 100 mL of potato dextrose broth (PDB, potato infusion of 200 g fresh potato, dextrose 15 g, distilled water 1.0 L, pH 7.0) at 130 rpm and 28°C for 3 days. Each 20-25 mL of seed culture was transferred into a 1.0 L Erlenmeyer flask containing 250 mL of PDB and incubated at 130 rpm and 28°C for 7 days.

1.3. Extraction and isolation of new compounds

The production culture (50 L) was centrifuged to separate the mycelia from the supernatant. The extracts of the fermentation broth and the mycelia were combined after TLC and HPLC analysis to yield crude extract (59 g).The residue was firstly subjected to CC (silica gel, $CHCl_3$/MeOH 100 : 0, 50 : 1, 20 :1, 10 : 1 and 3 : 1 (v/v))

to afford Fractions 1-5. Fr. 2 was fractioned by column chromatography on CC eluted with $CHCl_3$/MeOH(40:1) to give four subfractions (Fr. 2.1 - Fr. 2.4). The sub-fraction Fr.2.2 was eluted upon Sephadex LH-20 (methanol) to afford compound **1** (5 mg). Fr. 3 was fractioned by column chromatography on CC eluted with $CHCl_3$/MeOH (50:1, 20:1, 5:1) to give five subfractions (Fr. 3.1–Fr. 3.5). Fr.3.3 was further applied to CC (silica gel, petroleum ether/acetone 3:1) and finally by Sephadex LH-20 (methanol) to afford compounds **2** (3 mg). Fr. 3.4 was further applied to CC eluted with $CHCl_3$/MeOH (20:1) to afford compound **3** (5 mg), **6** (3 mg). Fr. 4 was further applied to CC (silica gel, $CHCl_3$/MeOH 20:1, 10:1, 5:1) to afford Fr. 4.1-Fr.4.4. Compound **4** (3 mg) and **5** (2 mg) was obtained from Fr. 4.2 by Sephadex LH-20 (methanol).

1.4. AChE inhibition assay

AChE inhibitory activities of the compounds were assayed by the spectrophotometric method developed by Ellman et al. with slight modification. S-acetylthiocholineiodide, S-butyrylthio choline iodide, 5,5'-dithio-bis-(2-nitrobenzoic) acid (DTNB, Ellman's reagent), and acetylcholinesterase derived from human erythrocytes were purchased from Sigma Chemical. The compounds were dissolved in DMSO. The reaction mixture (total volume of 200 μL) containing phosphate buffer (pH 8.0), a test compound (50 μM), and acetyl cholinesterase (0.02 U/mL), was incubated for 20 min (at 37 °C). Then, the reaction was initiated by adding 40 μL of the solution containing DTNB (0.625 mM) and acetylthiocholine iodide (0.625 mM). The hydrolysis of acetylthiocholine was monitored at 405 nm every 30 seconds for an hour. Tacrine (Sigma, purity > 99%) was used as a positive control with a final concentration of 0.333 μM. All the reactions were performed in triplicate. The percentage inhibition was calculated as follows: % inhibition = (E - S)/E × 100, where (E is the activity of the enzyme without a test compound, and S is the activity of the enzyme with a test compound).

1.5. NO inhibitory activity

The NO inhibitory activity of these compounds was determined using the Griess reagent assay for NO production. Briefly, the murine macrophage cell line was used as detection model. The supernatants were used to measure the NO production with an MTT [3-(4,5-dimethylthiazol-2-yl)-2,5-diphenyltetrazoliumbromide] assay for cell viability. L-NMMA was used as the positive control for ratio of inhibition at 52% with concentration at 50 μM.

1.6. Anticoagulation activity assay

The samples were dissolved in DMSO, and DMSO was used as a control group. Low molecular weight heparin (LMWH) was used as positive control for APTT at 79.7±0.36 s. For the activated partial thromboplastin time (APTT) assay, the plasma was mixed with compounds **3**, **6**, **4, 5** (100 mM) for 2 min at 37 °C. Then APTT assay reagent was added to the mixture and incubated for 3 min at 37 °C. Finally, 20 mM $CaCl_2$ was added, and the clotting time was recorded. All the results were expressed as mean ± standard deviation, three times in four channels. The *P*-values of less than 0.05 ($P < 0.05$) were considered significant.

1.7. Cytotoxicity assay

The cytotoxicity of compounds **1** and **2** against HL-60, SMMC-7721, A-549, MCF-7, and SW480 cell lines were determined in vitro by the 3-(4,5-dimethylthiazol-2-yl)-5(3-carboxymethoxyphenyl)-2-(4-sulfopheny)-2H-tetraz olium (MTS) method. Taxol was used as a positive control with IC_{50} <0.008 μM.

1.8. Photodynamic antimicrobial activity

Two Gram-positive bacteria (*B. subtilis*, *S. aureus*), a Gram-negative bacterium (*E. coli*), and a fungus (*C. albicans*) were selected for the antimicrobial activity assay. The *B. subtilis*, *S. aureus* and *E. coli* were cultured in LB broth medium to reach 1×10^5 CFU/mL. The *C. albicans* was cultured in steriled PDB broth medium and the test concentration was 1×10^3 spores/mL. The test compounds were dissolved in DMSO, and their final concentrations ranged from 512 to 0.25 mg/mL by using the

two fold serial dilution method. The wells containing test strains and diluted compounds were incubated at 28°C (4 days) for fungi and 37 °C (24 h) for bacteria. The culture suspension and DMSO were used as negative controls. The LED light was used to illuminate the culture suspension for 0.5 h. The MICs were determined with a spectrophotometer plate reader set at 450 nm and defined as the drug concentration at which the optical density was ≤ 50% of that of the test-compound-free culture. Kanamycin and nystatin were used as positive controls for antibacterial and antifungal assays, respectively.

1.9. Glucose uptake stimulating cell assay

3T3-L1 preadipocytes were grown and passaged in DMEM containing 25 mmol/L glucose plus 10% calf serum. For adipocyte differentiation, 2-day postconfluent cells were placed in 10% FBS-DMEM with 1 μmol/L dexamethasone, 0.5 mmol/L 1-methyl-3-isobutylxanthine, and 1 μg/mL insulin. After 3 days, the medium was changed to 10% FBS-DMEM containing 1 μg/mL insulin alone for 2 more days and was then replaced with 10% FBS-DMEM. Thereafter, the medium was changed every 2 days.

The differentiated 3T3-L1 adipocytes that were plated into 96-well plates were preincubated with FBS-DMEM containing 0.2% BSA for 12 hours and were then incubated with 25 μmol/L samples in medium. 0.1 μmol/L insulin or 10 μmol/L berberine was used as positive controls. 24 hours later, the medium was removed and its glucose concentrations were determined by the glucose oxidase method. The amount of glucose consumption was calculated by the glucose concentrations of blank wells subtracting the remaining glucose in the cell-plated wells. Insulin and berberine were used as positive controls for the consumption rates of glucose at 24.84±2.17 %, 24.64±1.26 %.

*2, 3-dihydro-2, 5-dihydroxyl-2-methylchromen-4-one (**1**).* $[\alpha]_D^{20}$ 9.4 ($CHCl_3$); ^1H NMR (400 MHz) and ^{13}C NMR (100 MHz) see Table S1. HR-ESIMS m/z 177.555 $[M-H_2O+H]^+$(Calcd for $C_{10}H_9O_3$177.552).

*(2R, 4S)-2,3-dihydro-2-methyl-benzopyran-4,5-diol (**2**).* $[\alpha]_D^{25}$ 43.2 ($CHCl_3$);^{1}H NMR (400 MHz) and ^{13}C NMR (100MHz) see Table S1. HR-ESIMS m/z 179.0711 $[M-1]^-$(Calcd for $C_{10}H_{11}O_3$179.0708).

*(R)-3-methoxyl -1-(2,6-dihydroxyphenyl)-butan-1-one (**3**).* $[\alpha]_D^{25}$ -146.4($CHCl_3$); ^{1}H NMR (400 MHz) and ^{13}C NMR (100 MHz) see Table S1.HR-ESIMS m/z 233.0787 (Calcd for $C_{11}H_{14}O_4Na$ 233.0790).

*7-O-α-D-ribosyl-5-hydroxy-2-methyl-4H-chromen-4-one (**4**).* $[\alpha]_D^{25}$ 57.0 (MeOH); ^{1}H NMR (400 MHz) and ^{13}C NMR (100 MHz) see Table S2. HR-ESIMS m/z 347.0800 (Calcd for $C_{15}H_{16}O_8Na$ 347.0743).

*7-O-α-D-ribosyl-2,3-dihydro-5-hydroxy-2-methyl-chromen-4-one (**5**).* $[\alpha]_D^{25}$ 189.9 (MeOH); ^{1}H NMR (400 MHz) and ^{13}C NMR (100 MHz) see Table S2. HR-ESIMS m/z 349.0898 (Calcd for $C_{15}H_{18}O_8Na$ 349.0899).

*Daldinium A (**6**).* $[\alpha]_D^{25}$ 0 (MeOH); ^{1}H NMR (500 MHz) and ^{13}C NMR (125MHz) see Table S2. HR-ESIMS m/z 185.0819 (Calcd for $C_9H_{13}O_4$ 185.0814).

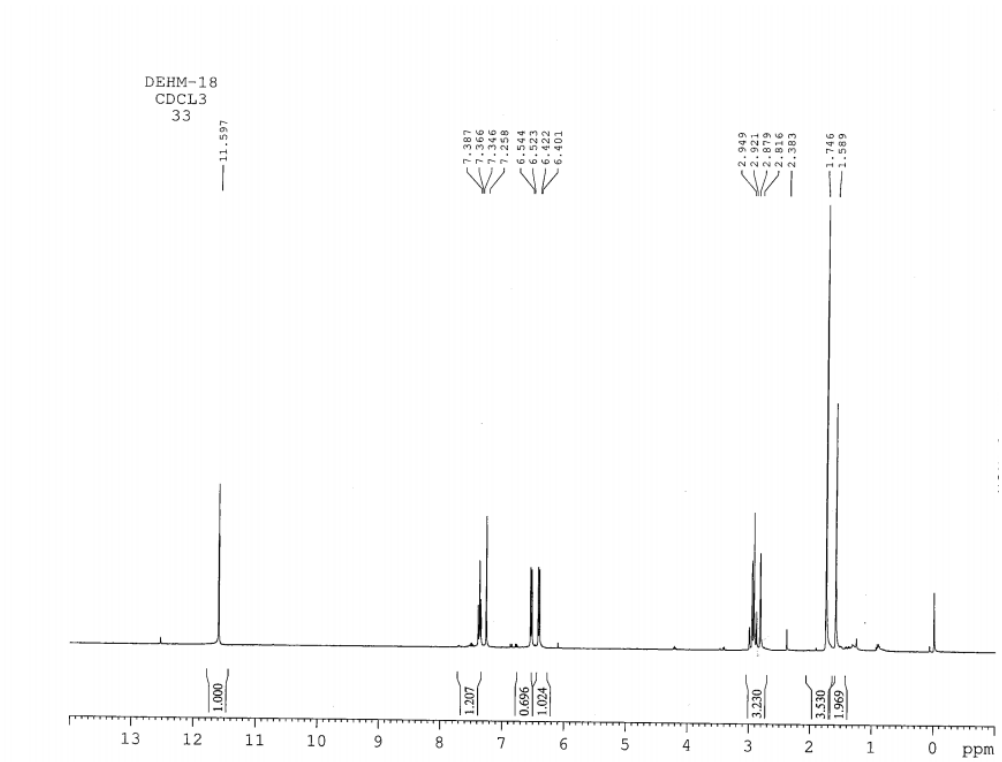

Figure S1. ^{1}H NMR of compound **1**

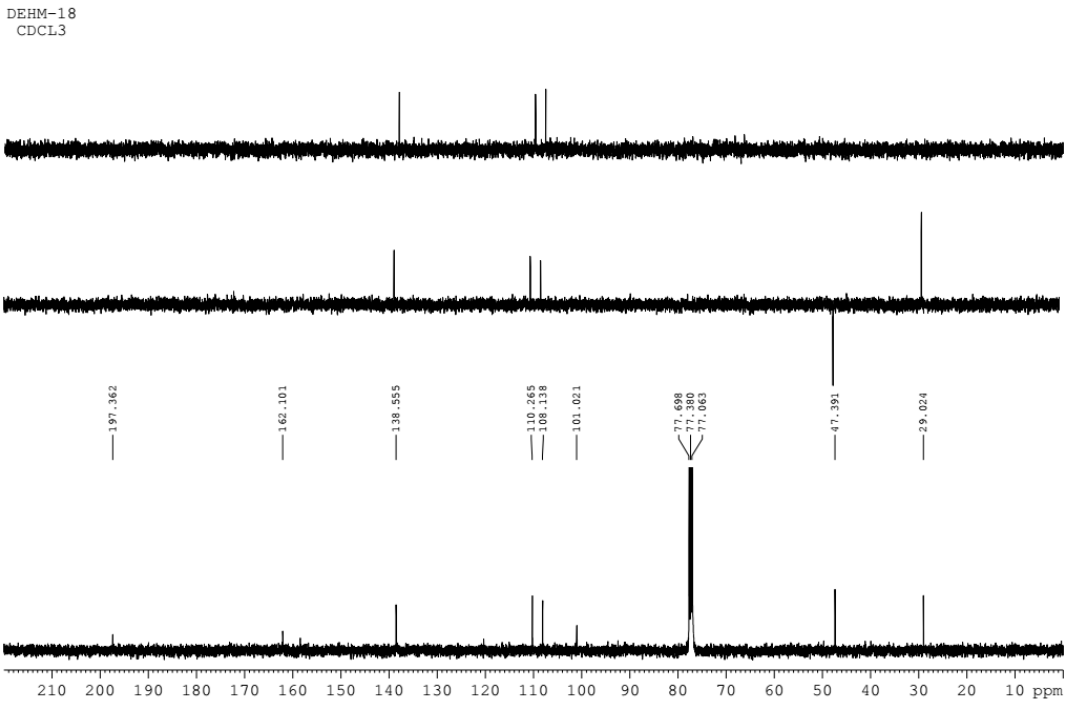

Figure S2. ^{13}C NMR of compound **1**

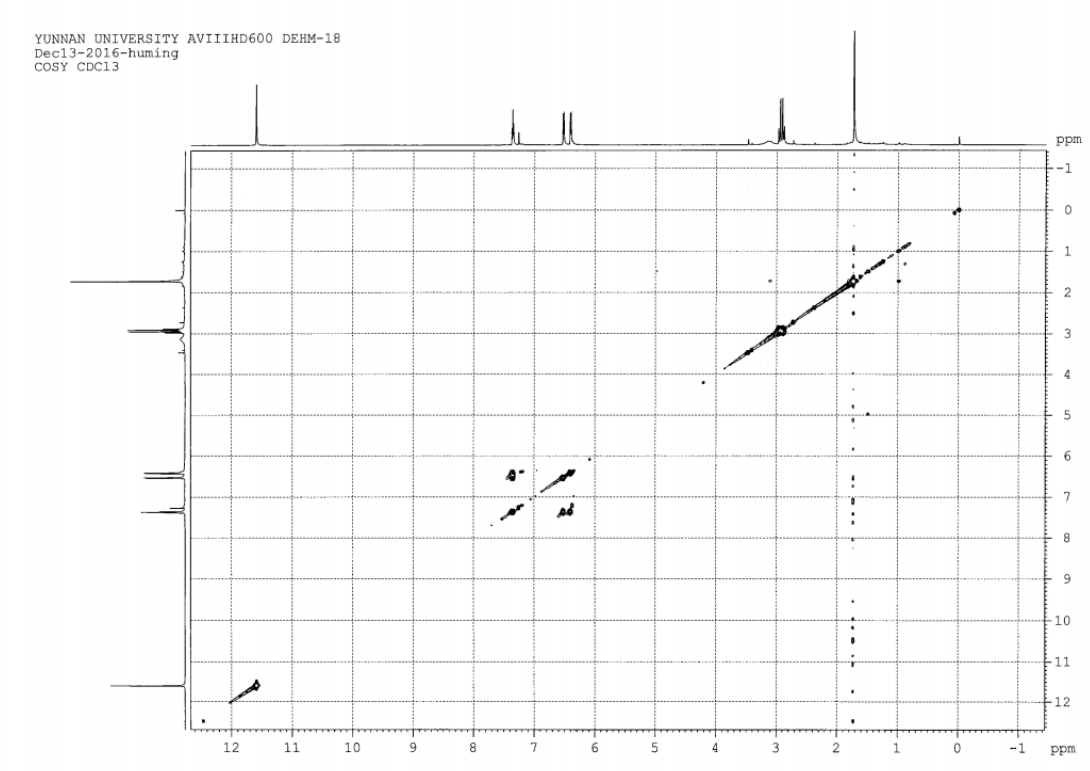

Figure S3. ^{1}H-^{1}H COSY Spectrum of compound **1** in $CDCl_3$

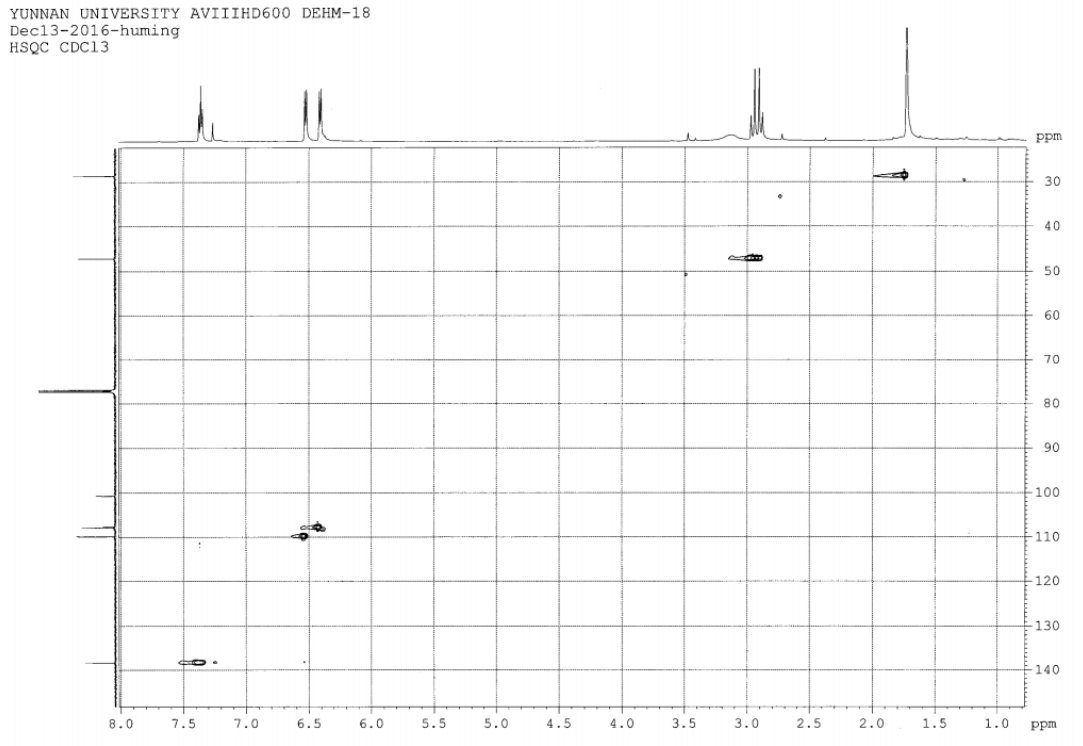

Figure S4. HSQC Spectrum of compound **1**in $CDCl_3$

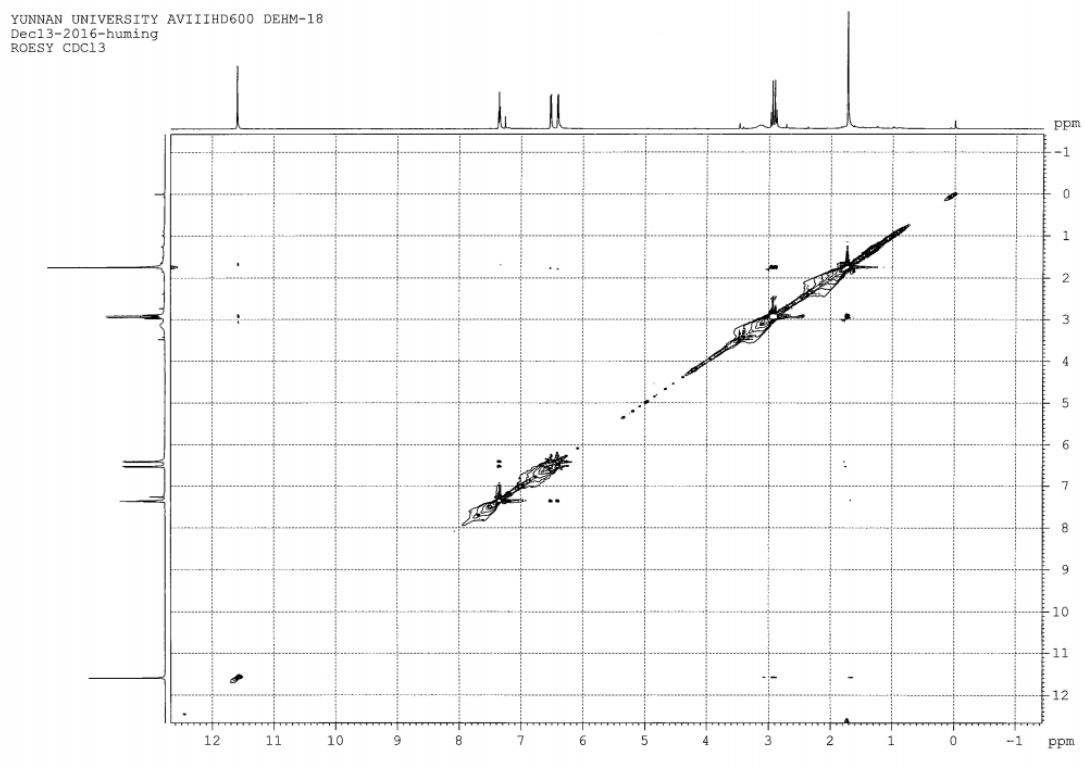

Figure S5. ROESY Spectrum of compound **1**in $CDCl_3$

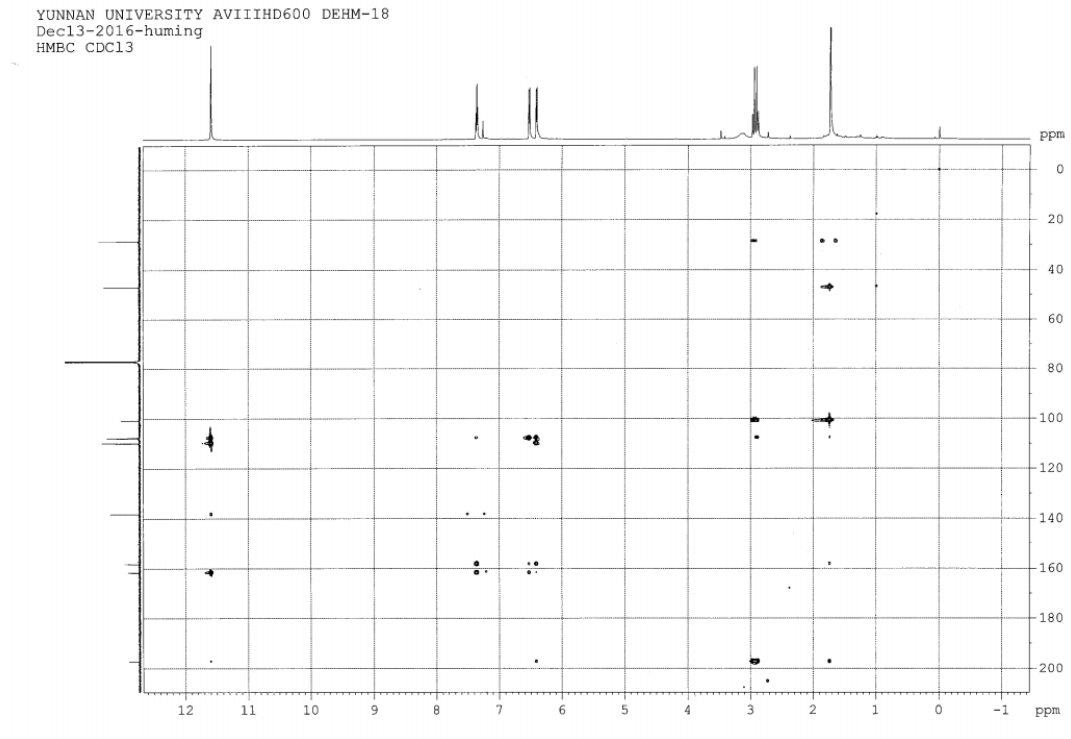

Figure S6. HMBC Spectrum of compound **1** in $CDCl_3$

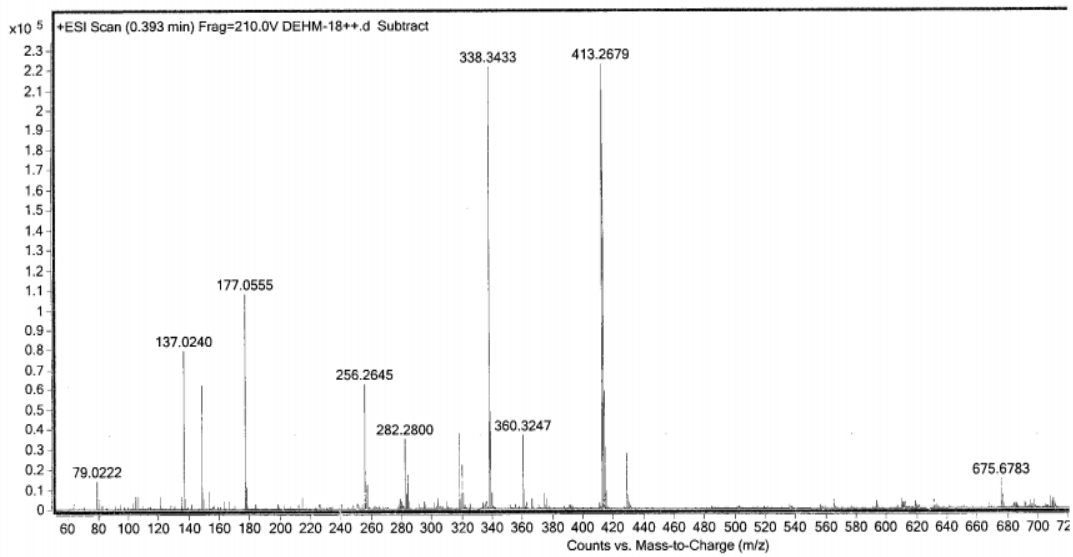

Figure S7. HR-ESIMS Spectrum of compound **1** in $CDCl_3$

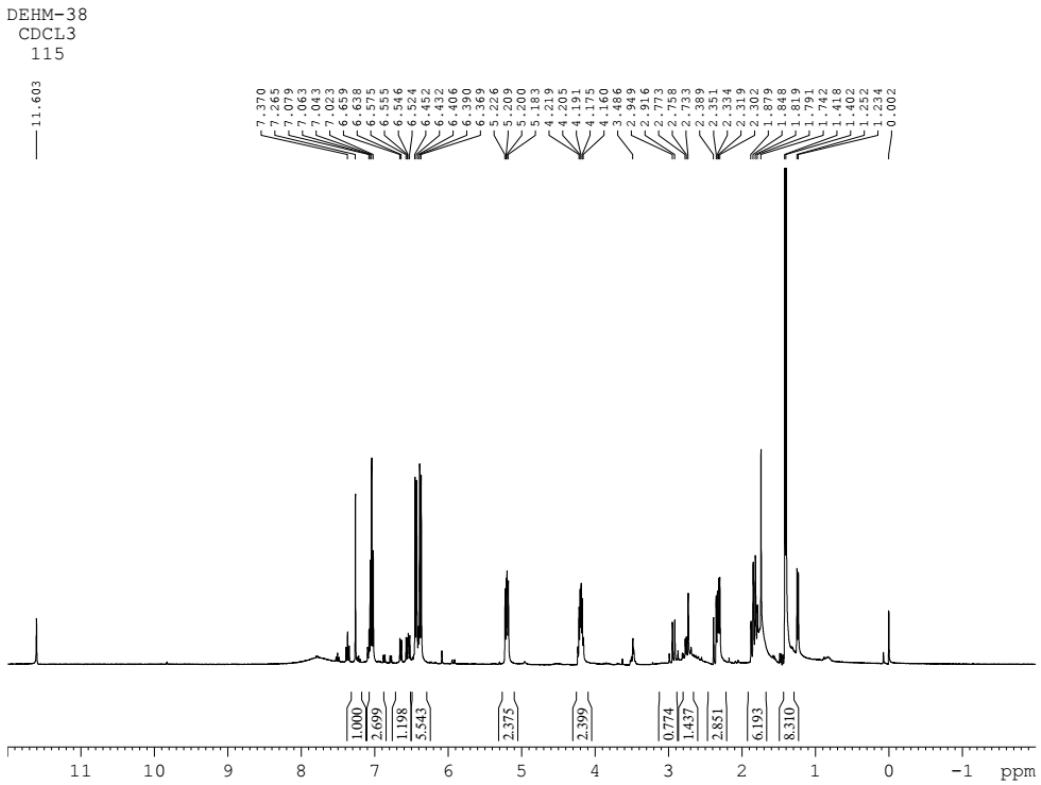

Figure S8. ^{1}H NMR of compound **2**

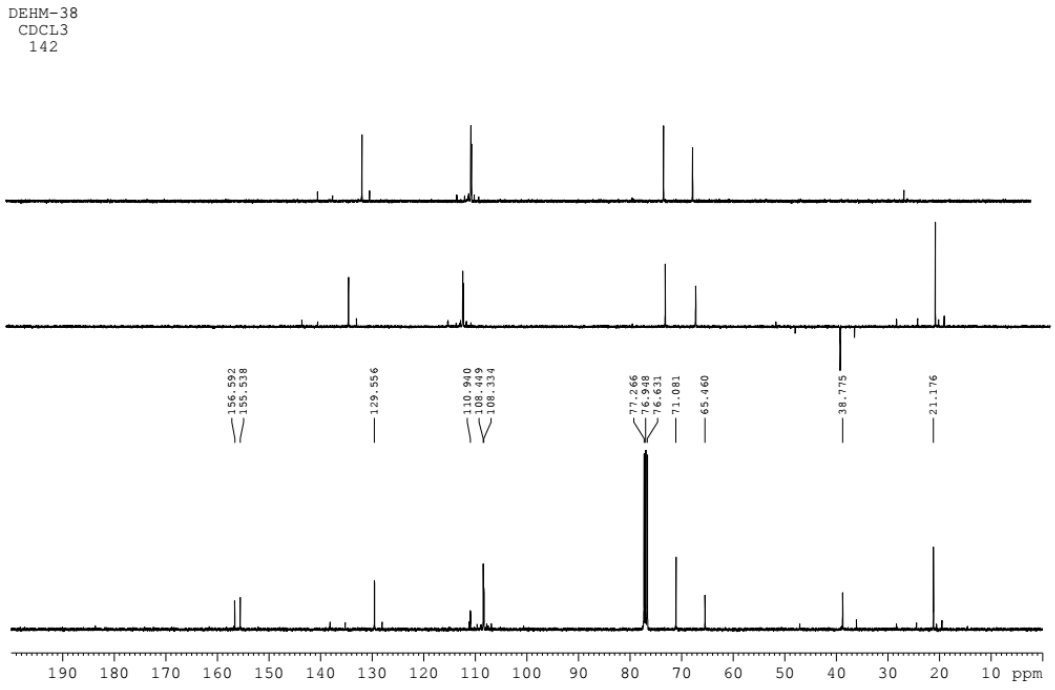

Figure S9. ^{13}C NMR of compound **2**

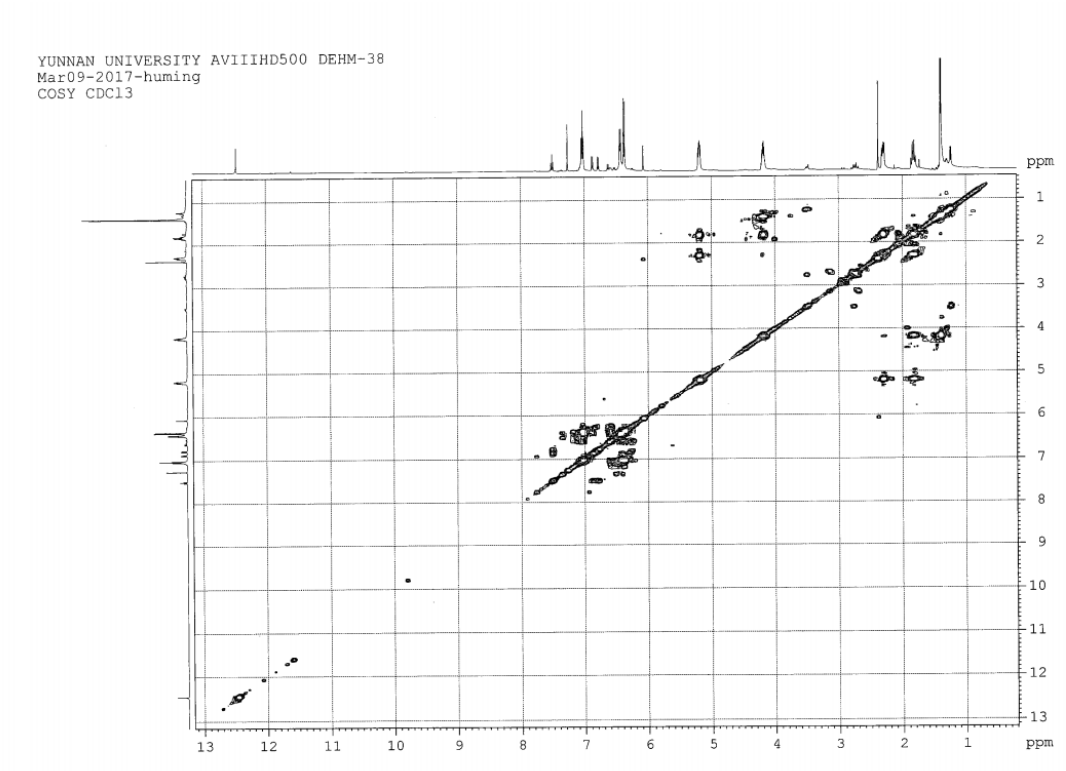

Figure S10. ^{1}H-^{1}H COSY Spectrum of compound **2** in $CDCl_3$

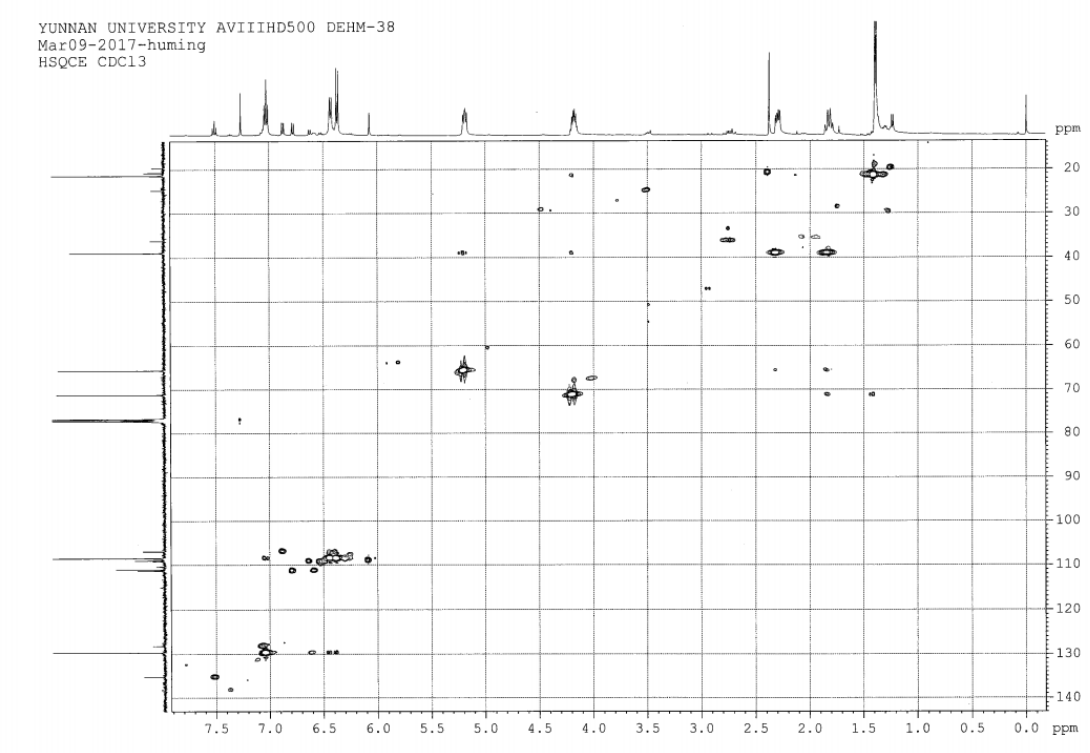

Figure S11. HSQC Spectrum of compound **2** in $CDCl_3$

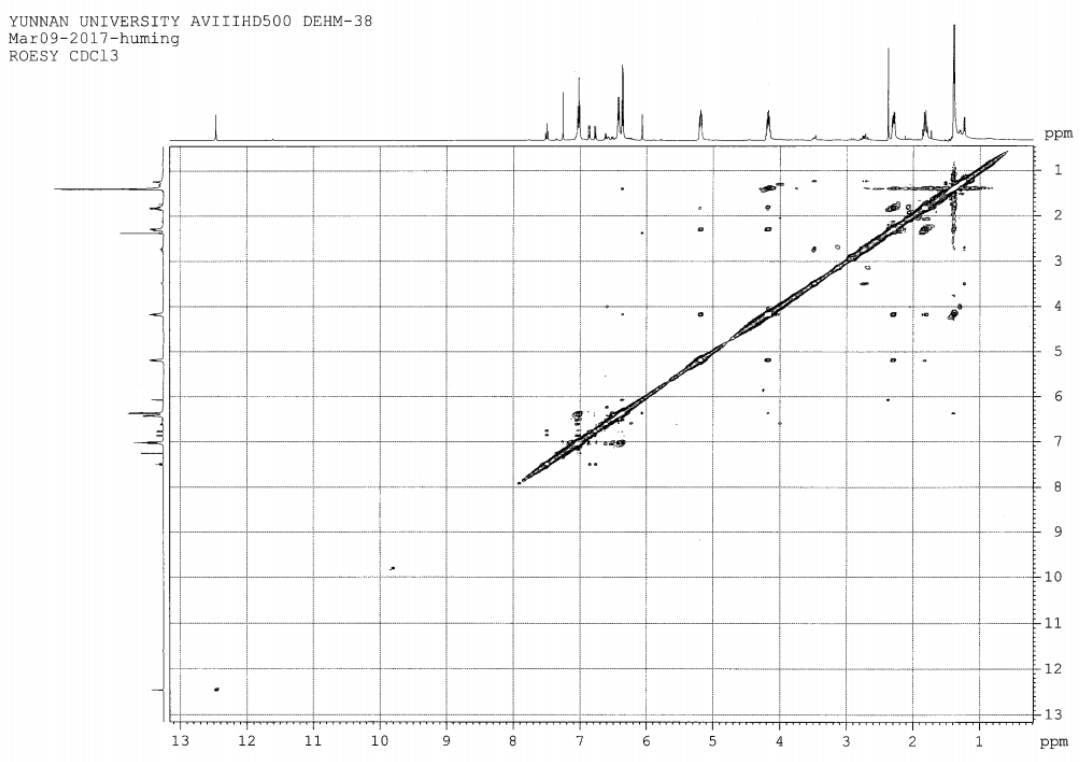

Figure S12. ROESY Spectrum of compound **2** in $CDCl_3$

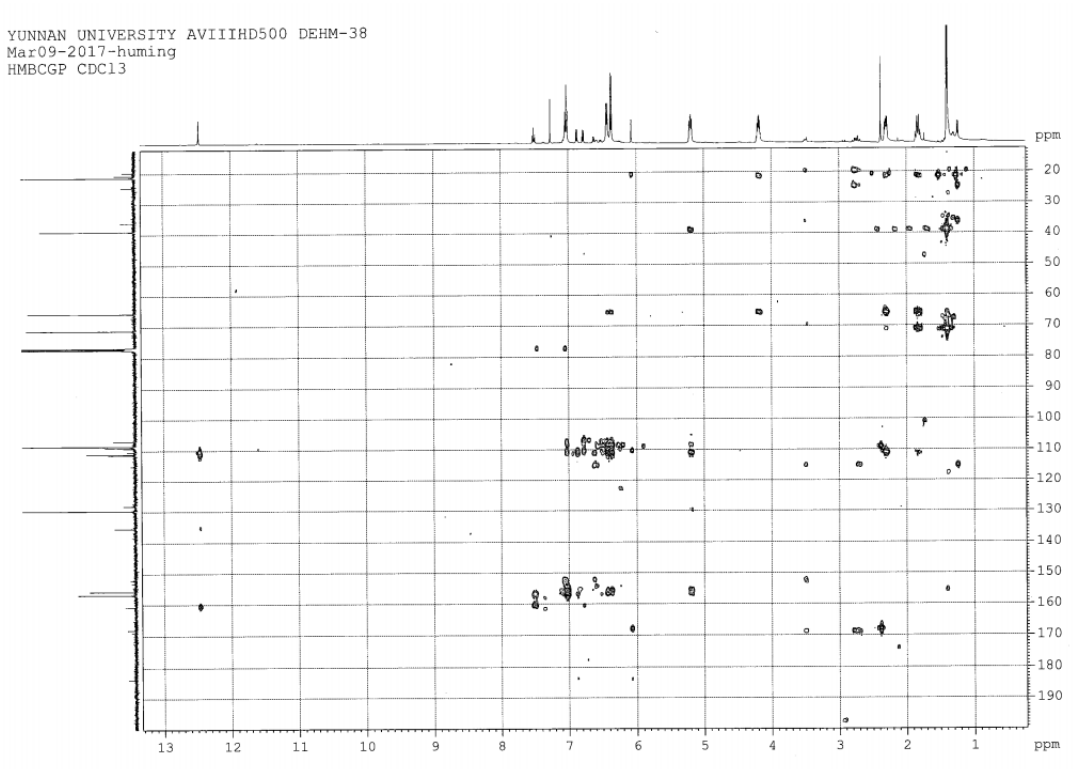

Figure S13. HMBC Spectrum of compound **2** in CDCL3

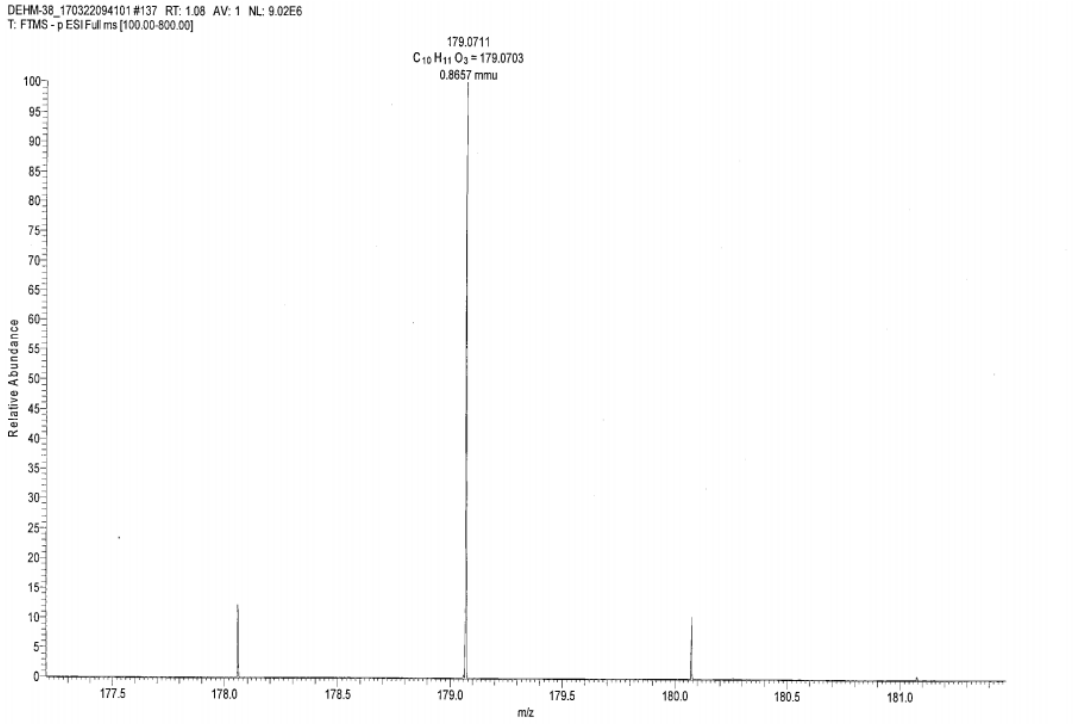

Figure S14. HRESIMS Spectrum of compound **2** in $CDCl_3$

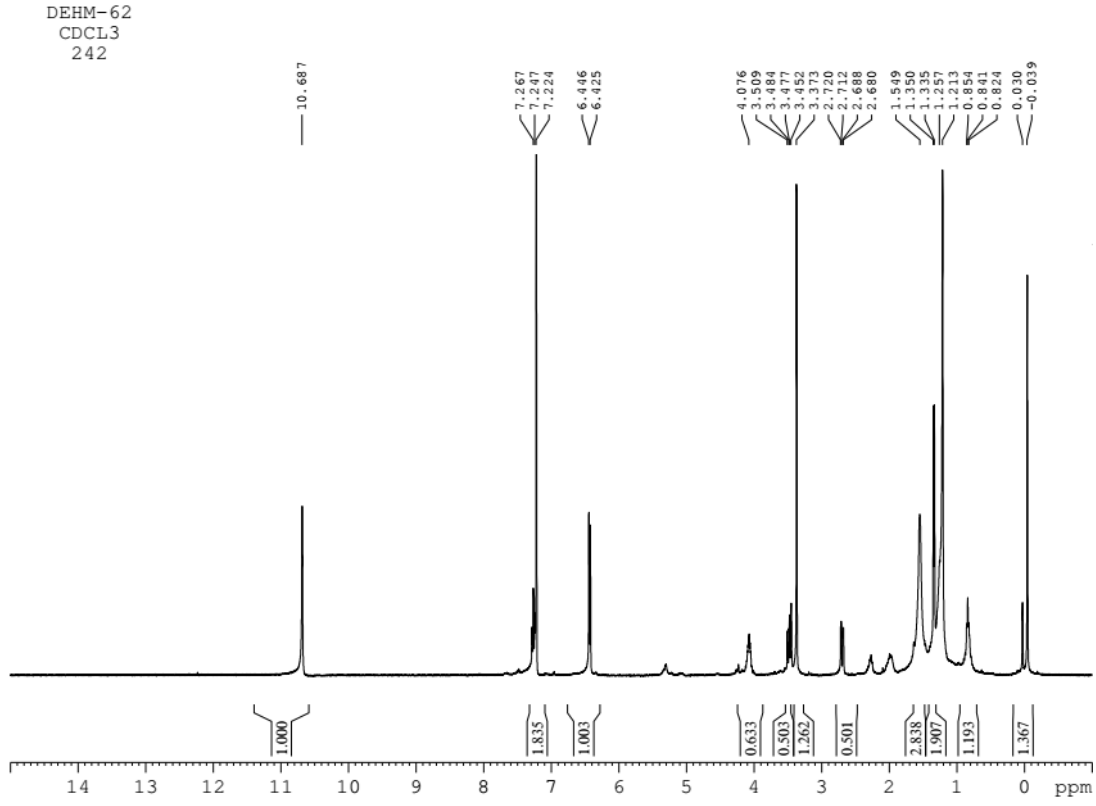

Figure S15. ^{1}H NMR of compound **3**

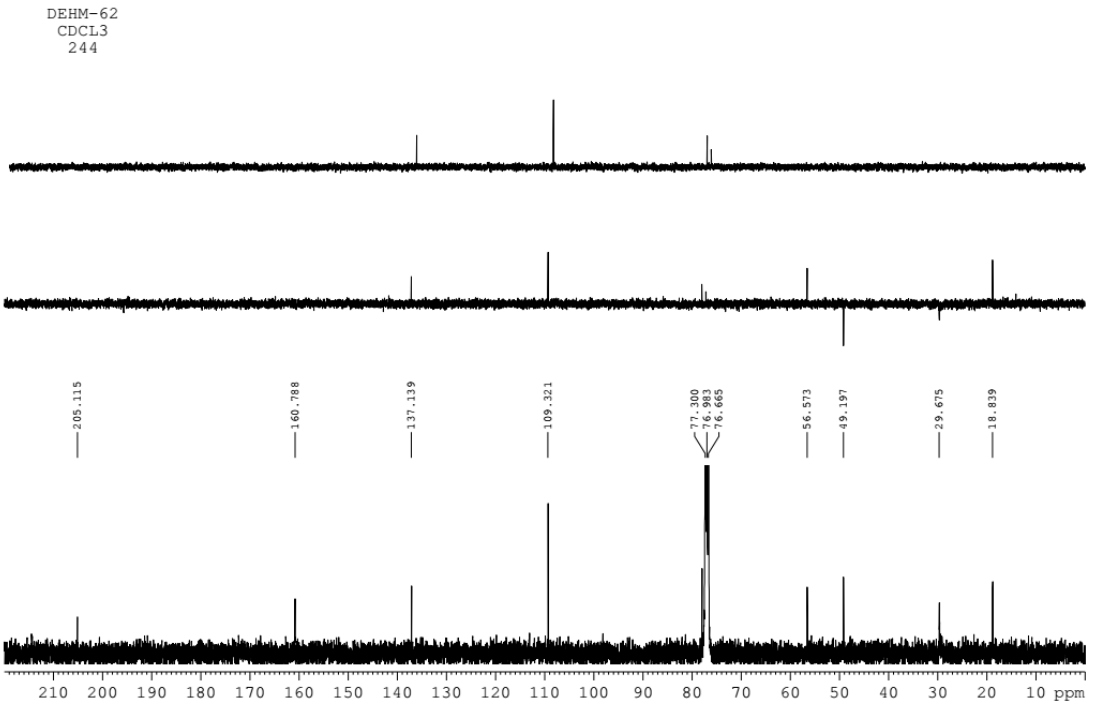

Figure S16. ^{13}C NMR of compound **3**

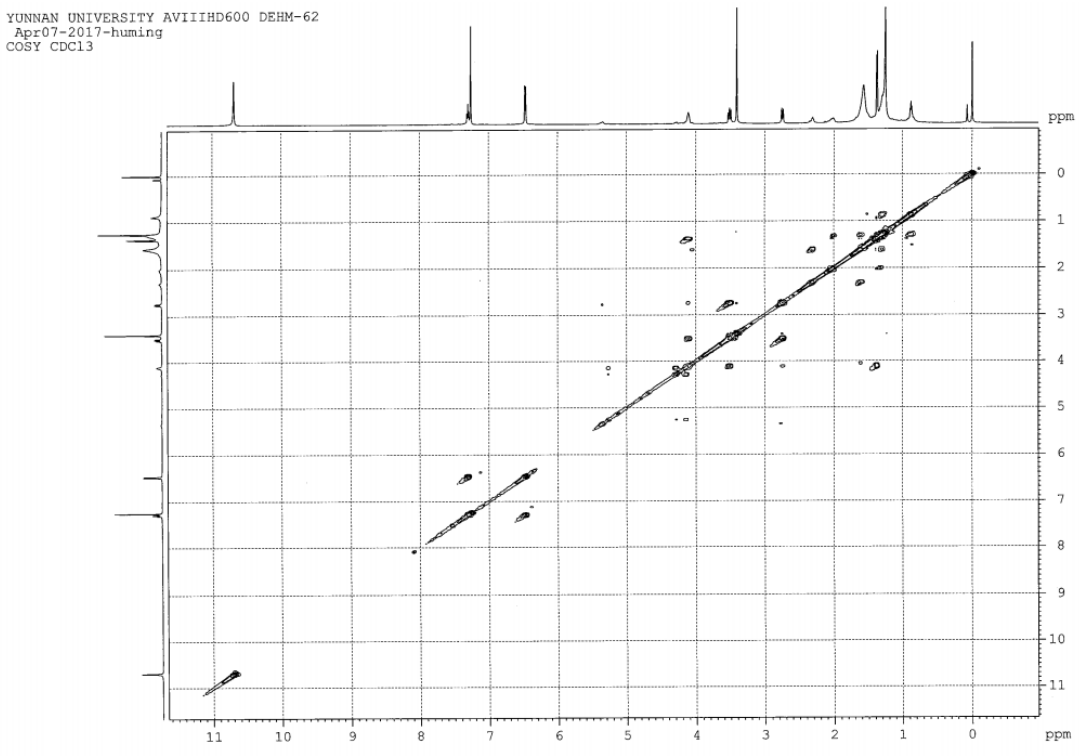

Figure S17. ^{1}H-^{1}H COSY Spectrum of compound **3** in $CDCl_3$

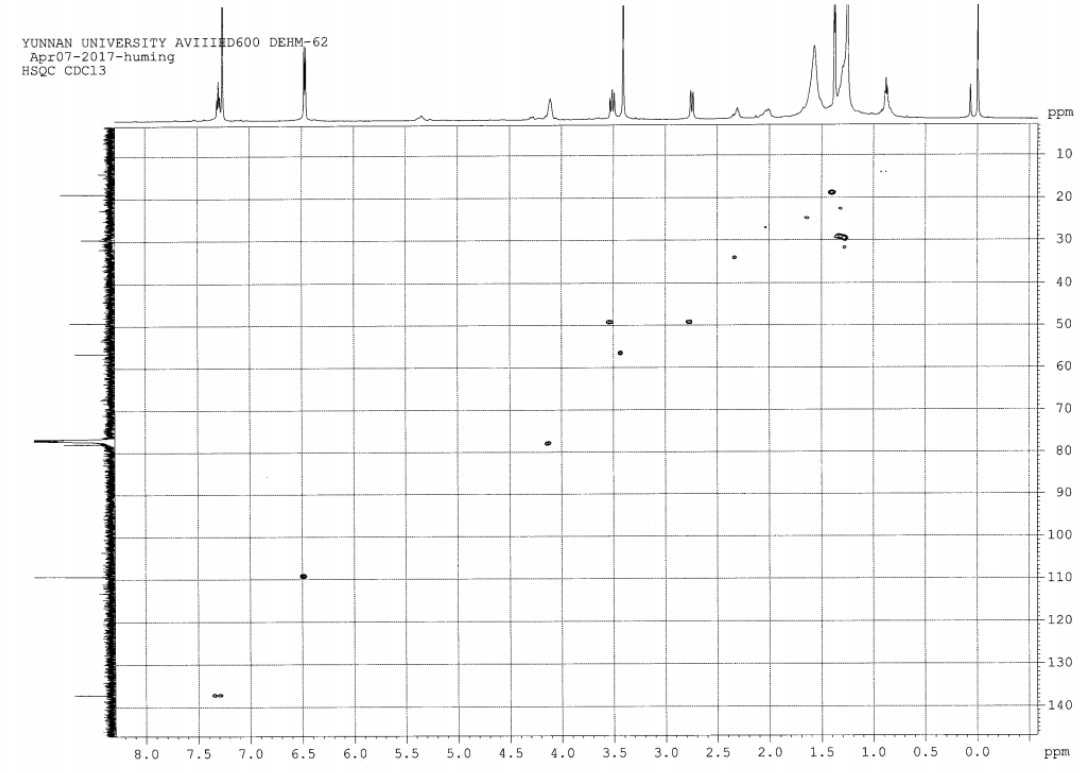

Figure S18. HSQC Spectrum of compound **3** in $CDCl_3$

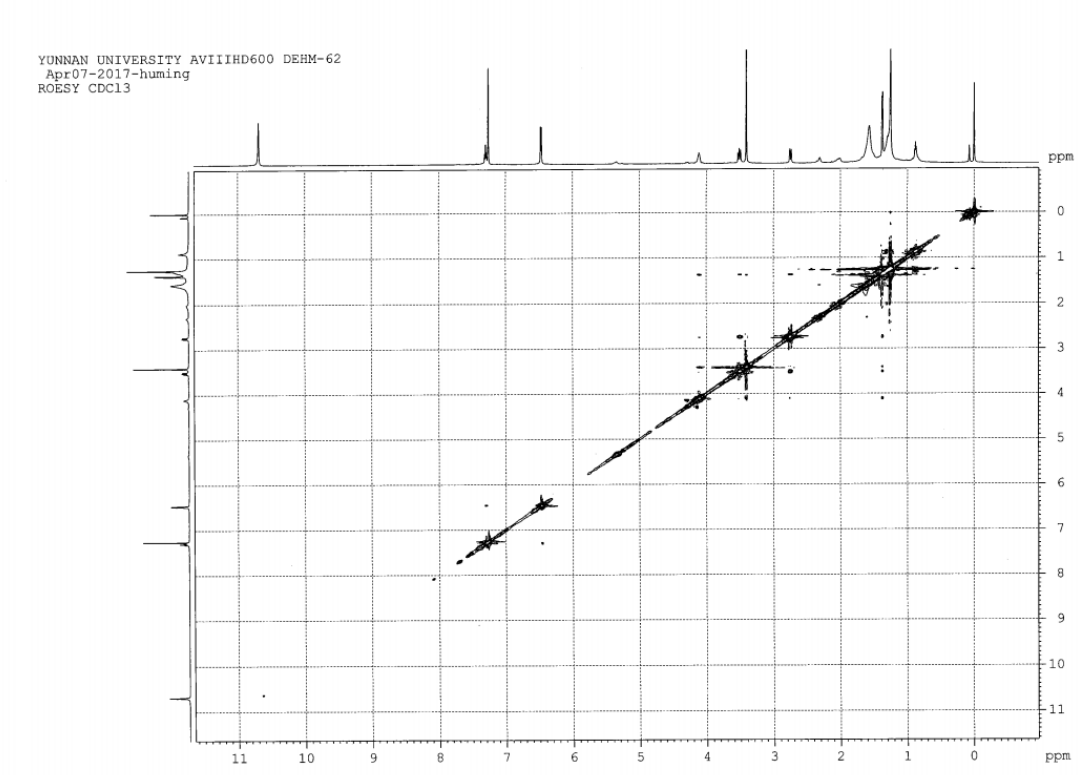

Figure S19. ROESY Spectrum of compound **3** in $CDCl_3$

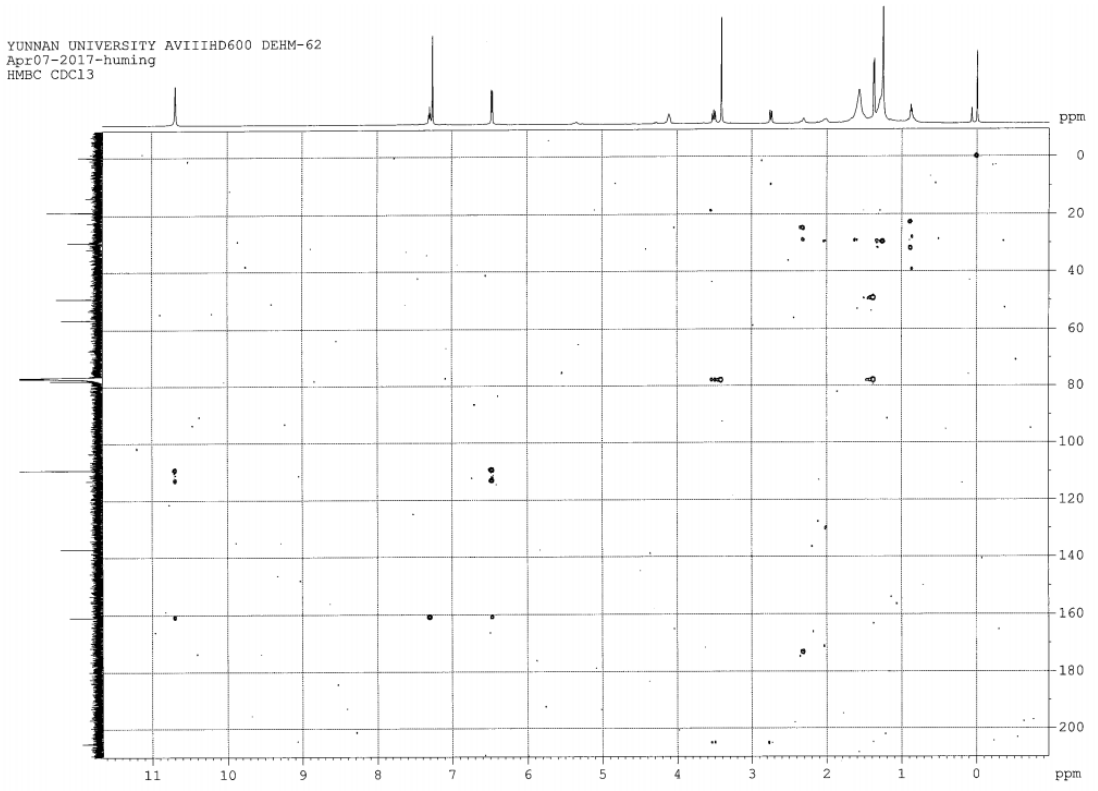

Figure S20. HMBC Spectrum of compound **3** in $CDCl_3$

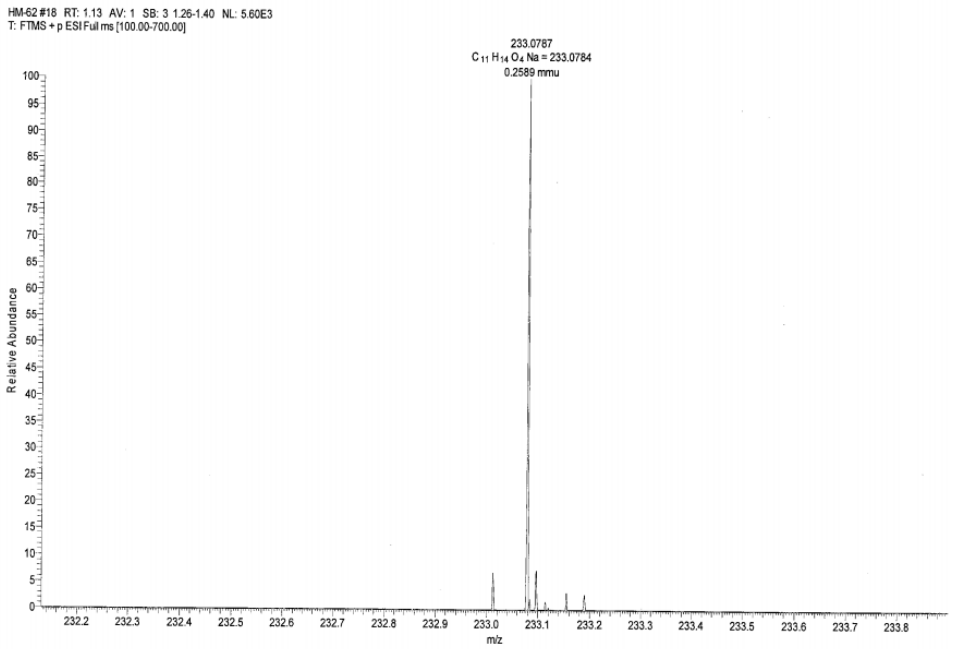

Figure S21. HRESIMS Spectrum of compound **3** in $CDCl_3$

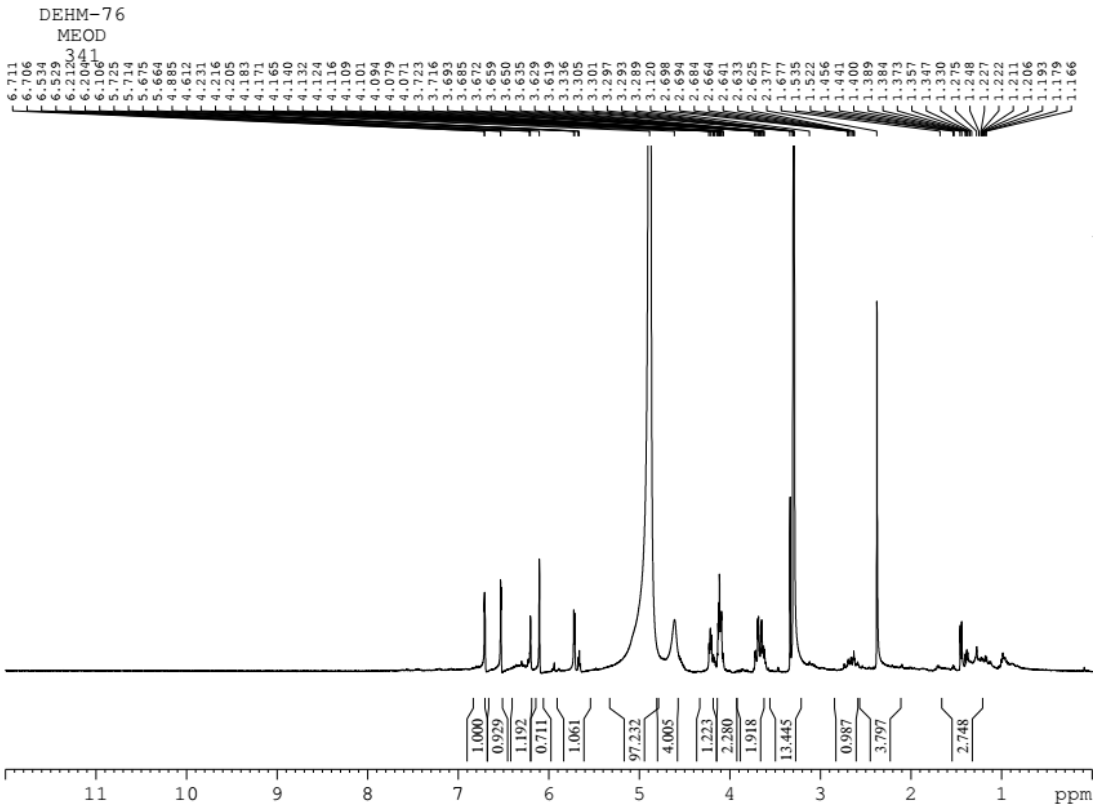

Figure S22. ^{1}H NMR of compound **4**

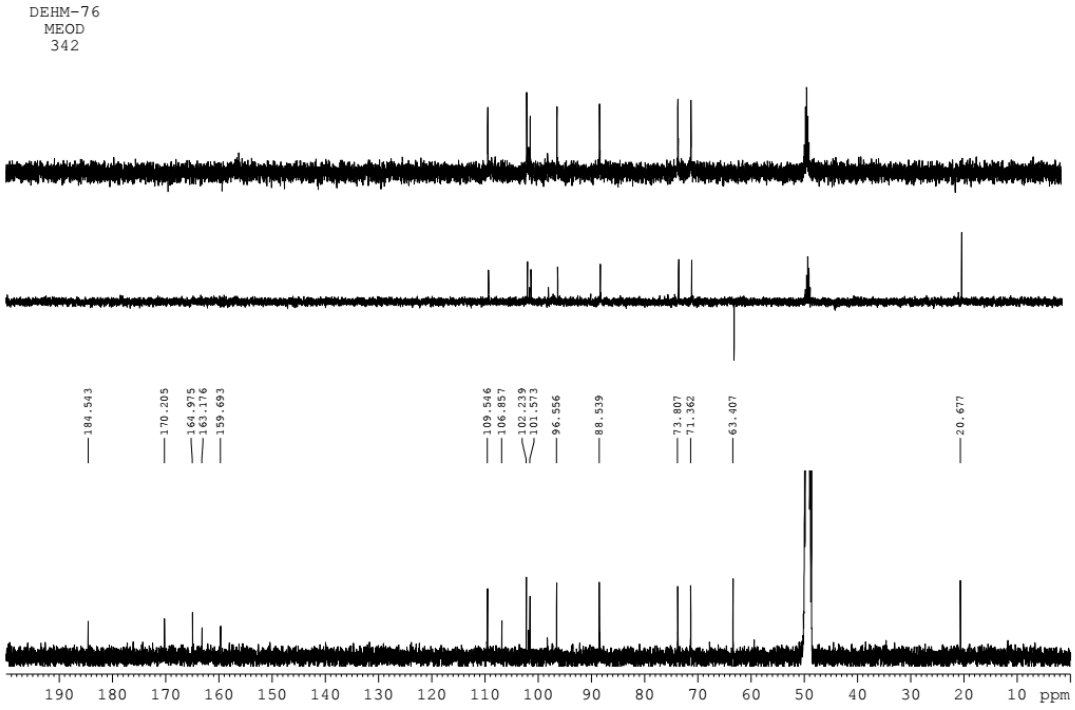

Figure S23. ^{13}C NMR of compound **4**

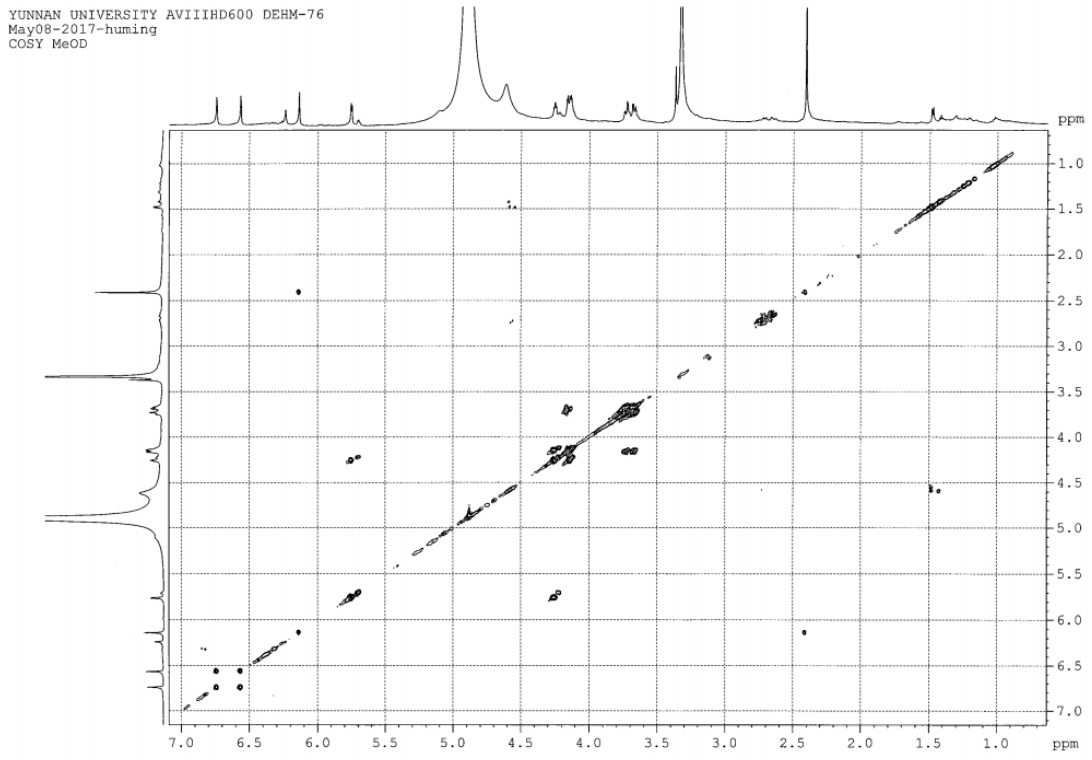

Figure S24. ^{1}H-^{1}H COSY Spectrum of compound **4** in MeOD

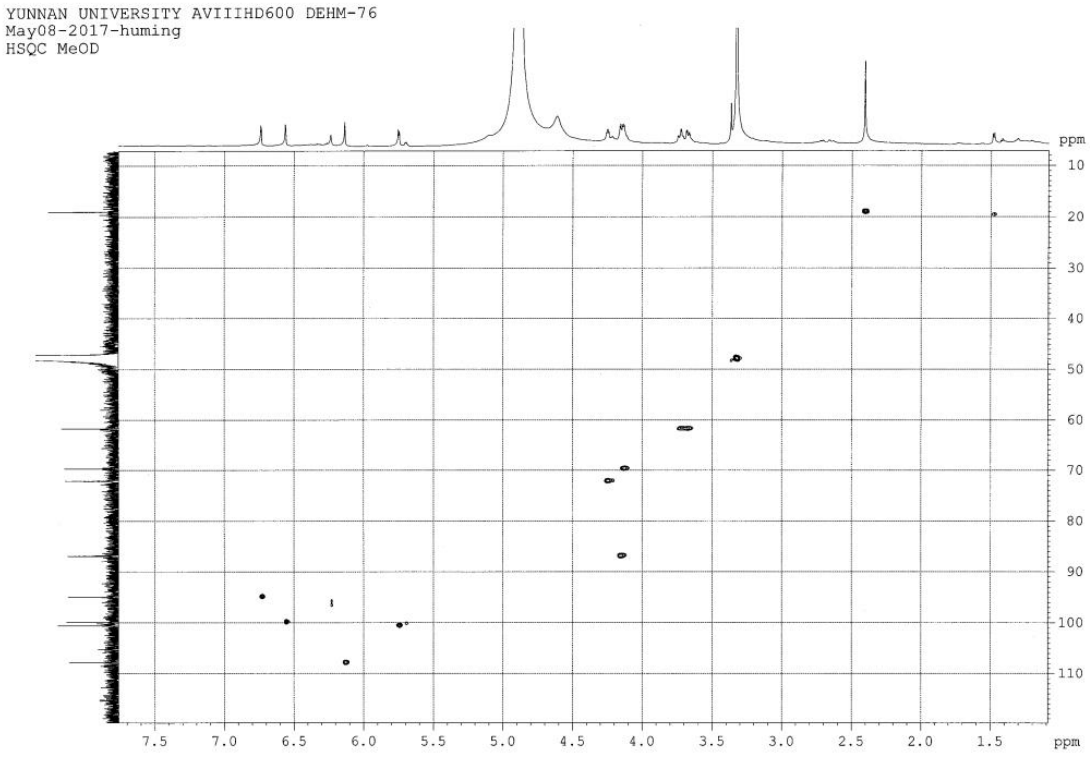

Figure S25. HSQC Spectrum of compound **4** in MeOD

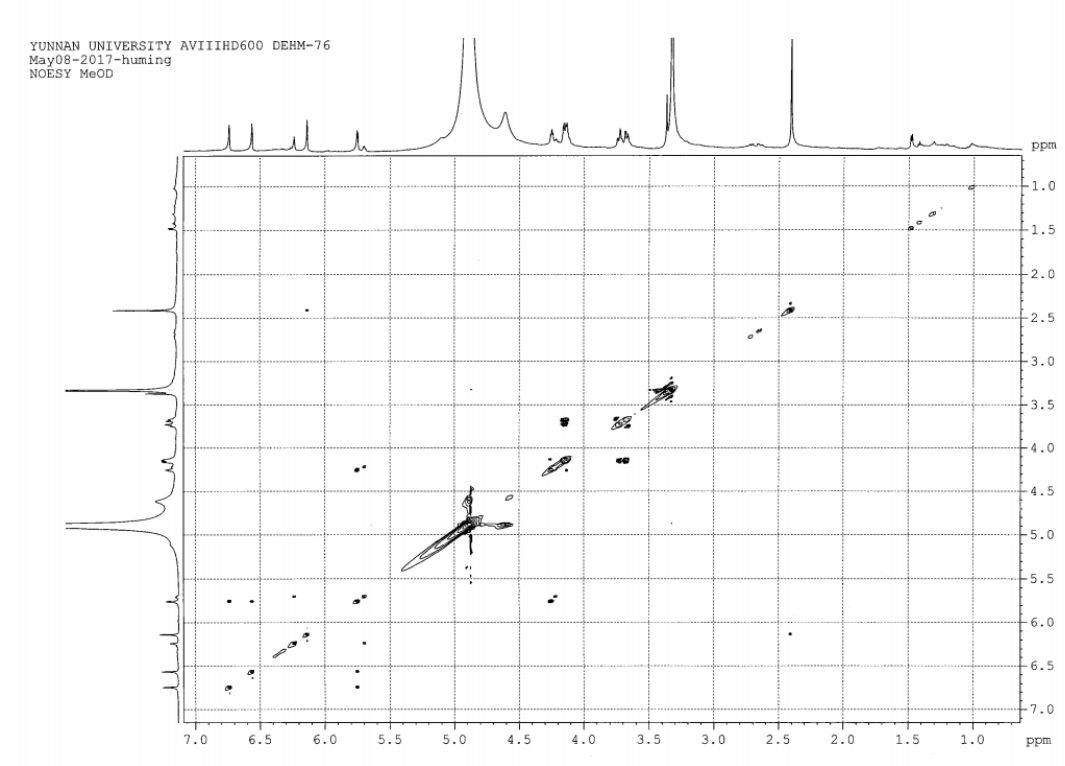

Figure S26. ROESY Spectrum of compound **4** in MeOD

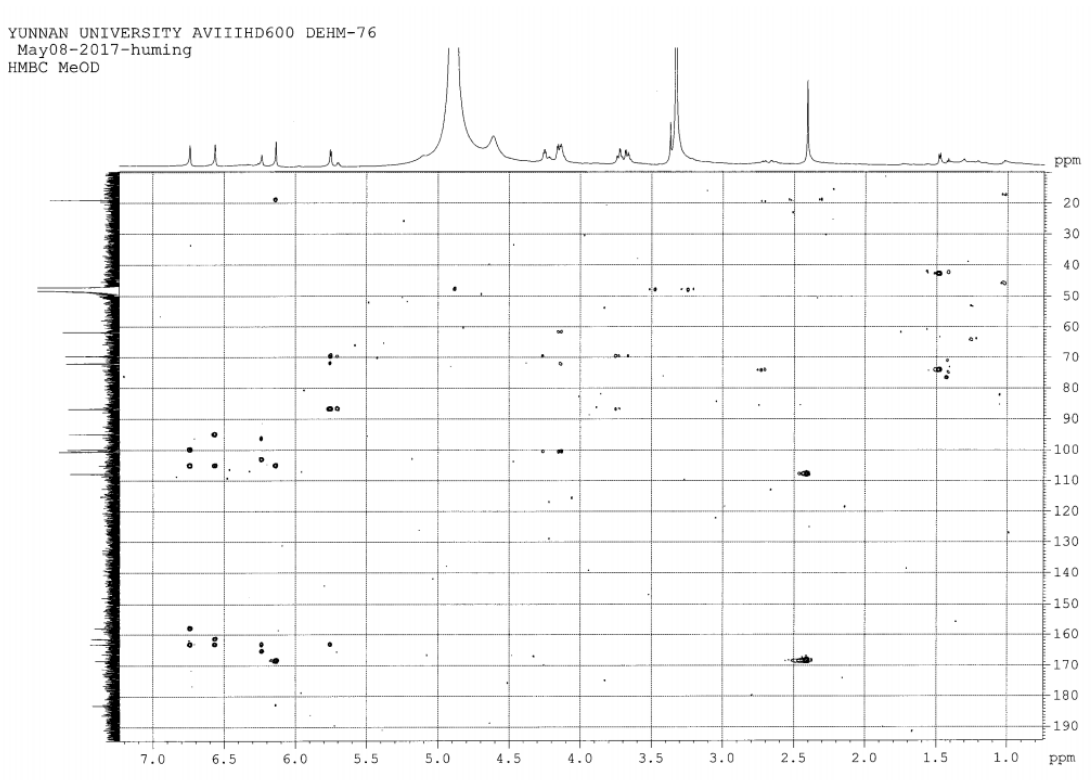

Figure S27. HMBC Spectrum of compound **4** in MeOD

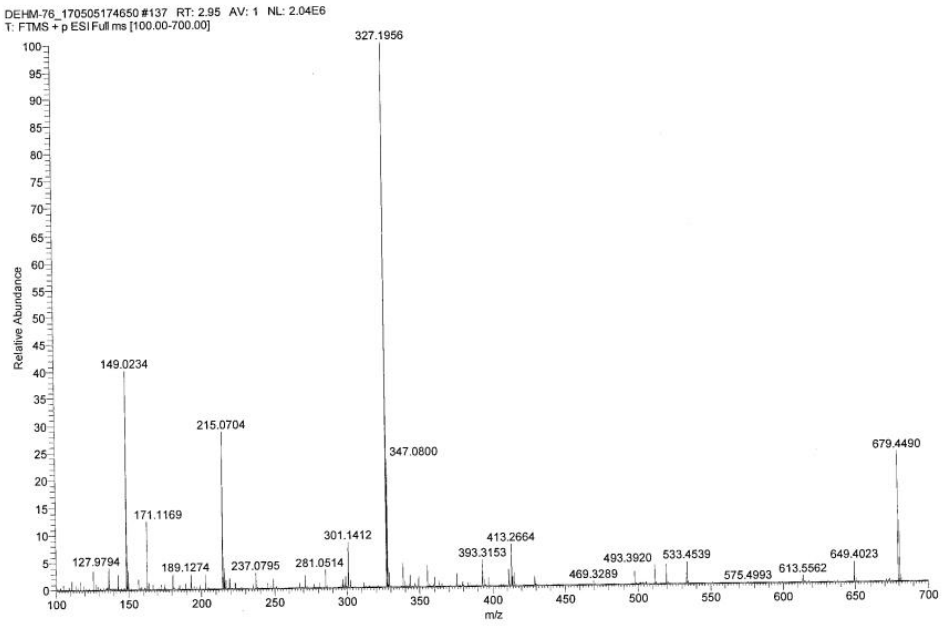

Figure S28. HRESIMS Spectrum of compound **4**

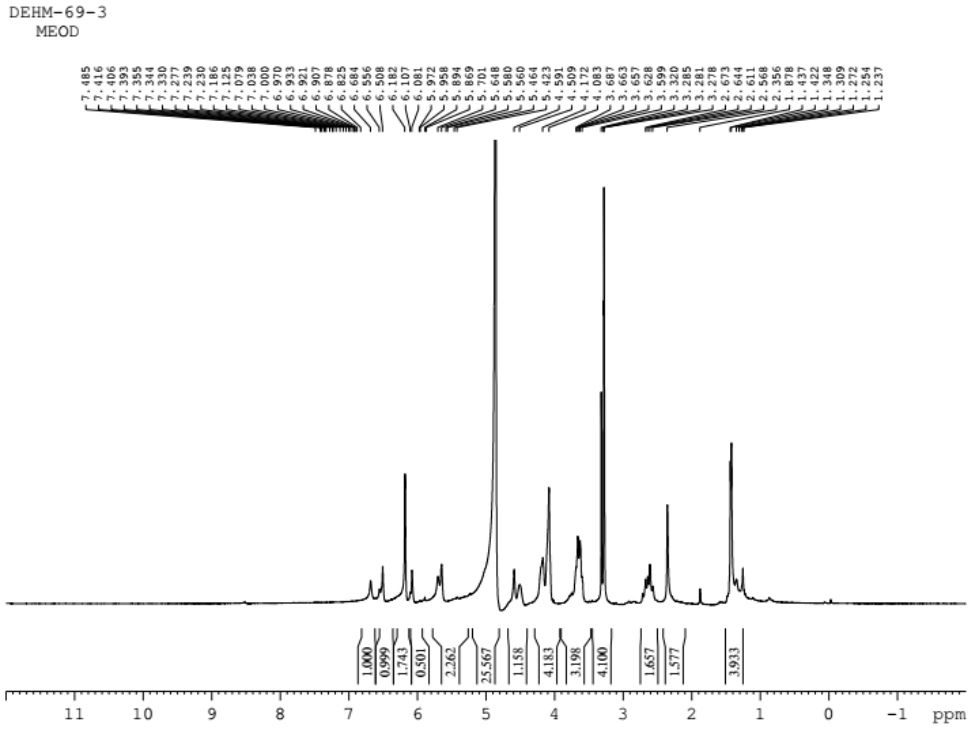

Figure S29. ^{1}H NMR of compound **5**

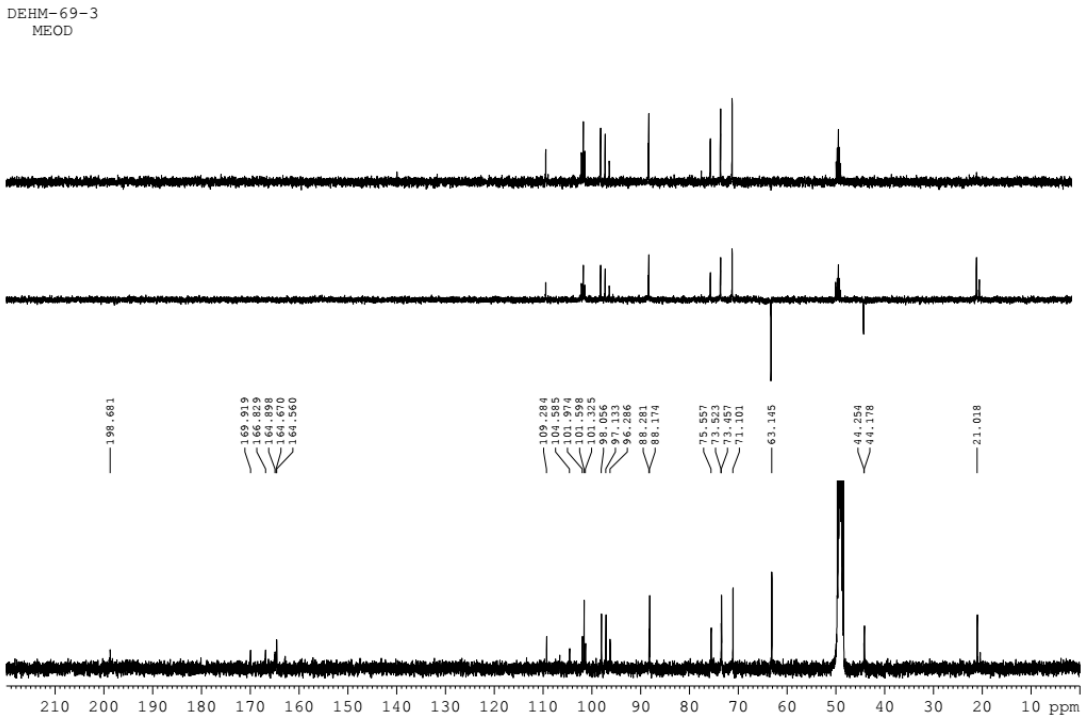

Figure S30. ^{13}C NMR of compound **5**

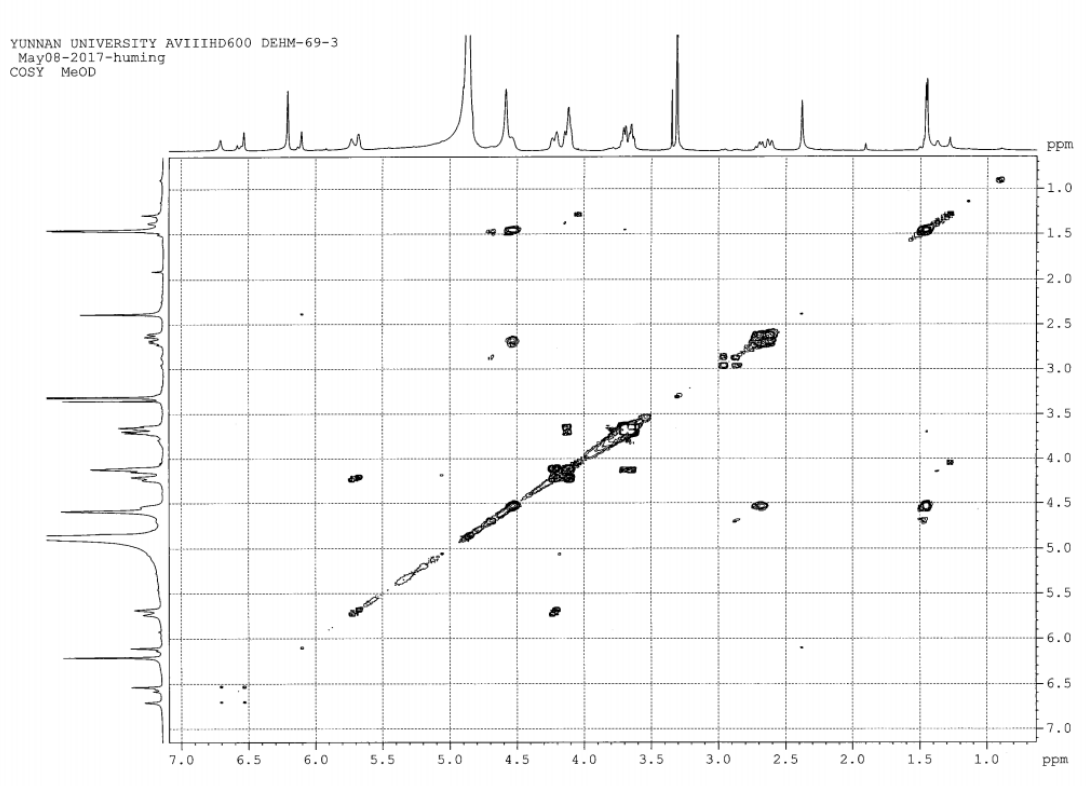

Figure S31. ^{1}H-^{1}H COSY Spectrum of compound **5** in MeOD

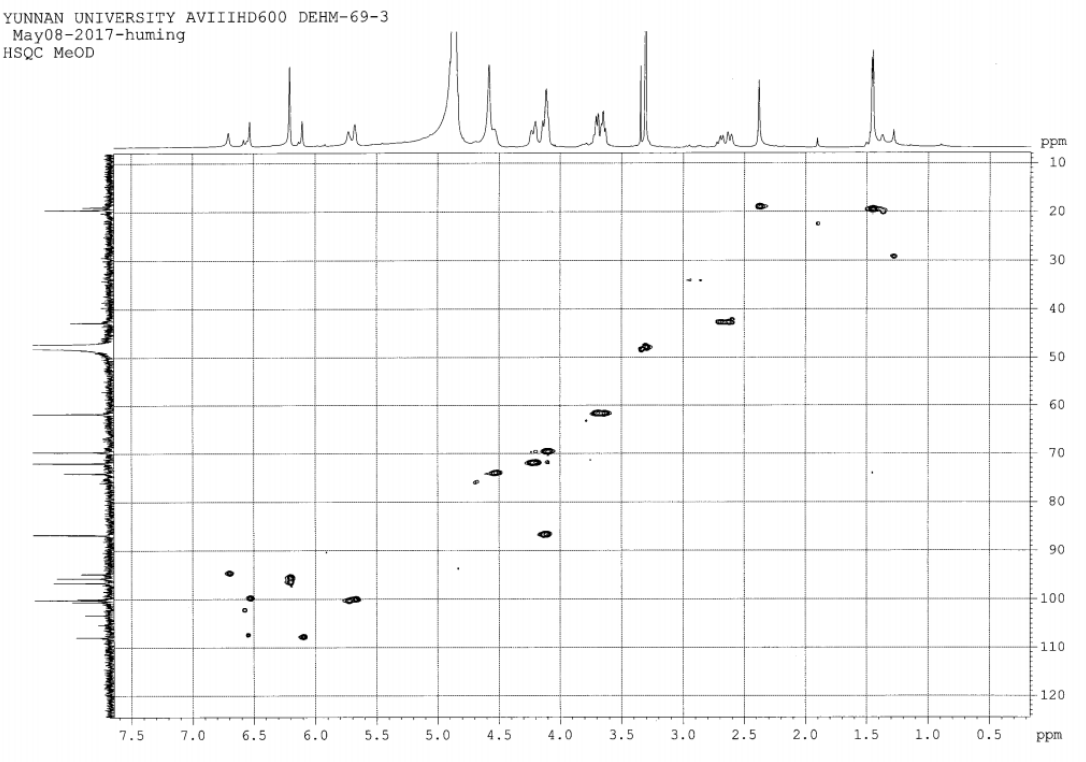

Figure S32. HSQC Spectrum of compound **5** in MeOD

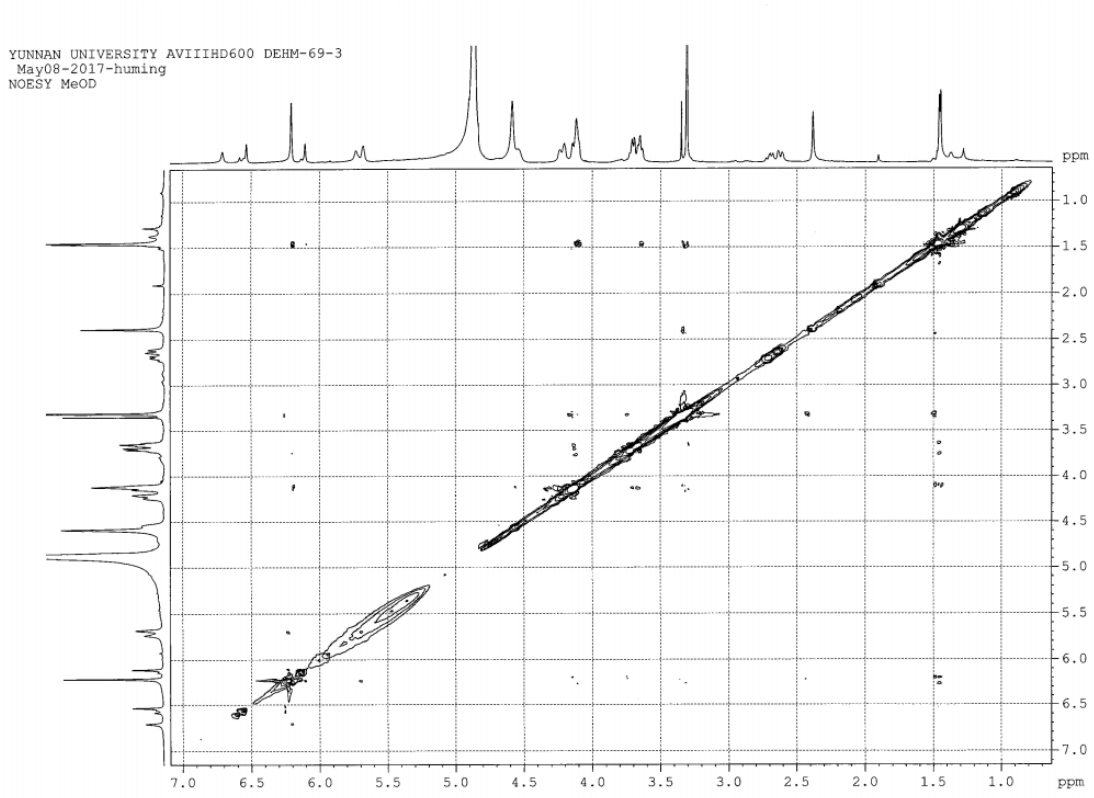

Figure S33. ROESY Spectrum of compound **5** in MeOD

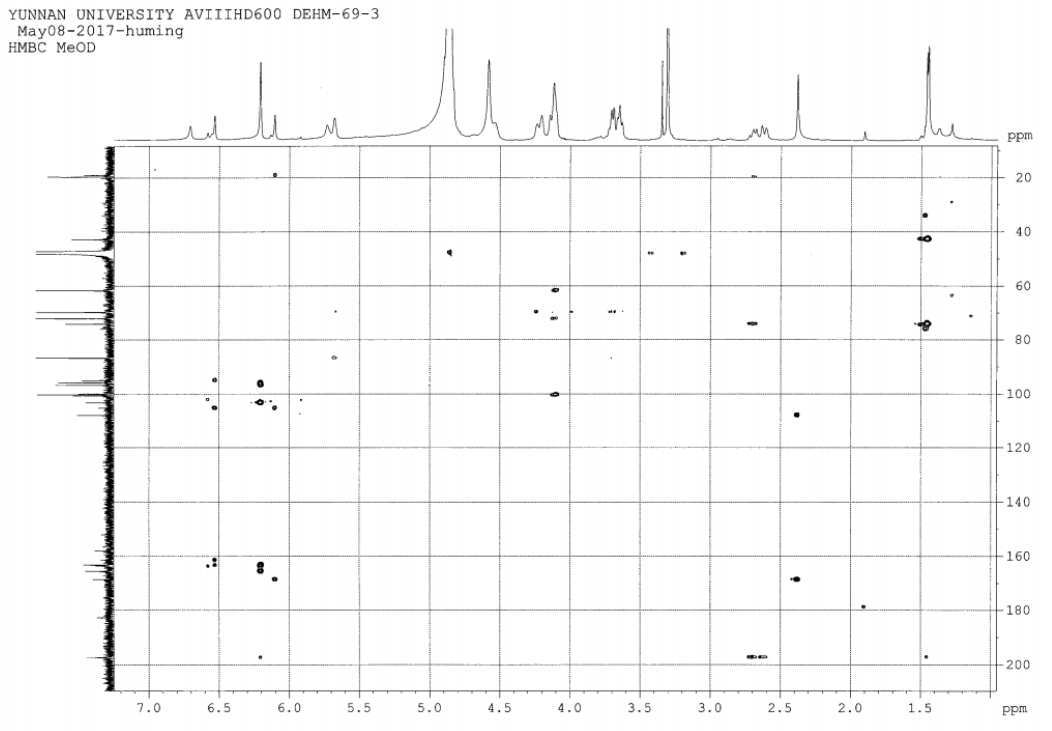

Figure S34. HMBC Spectrum of compound **5** in MeOD

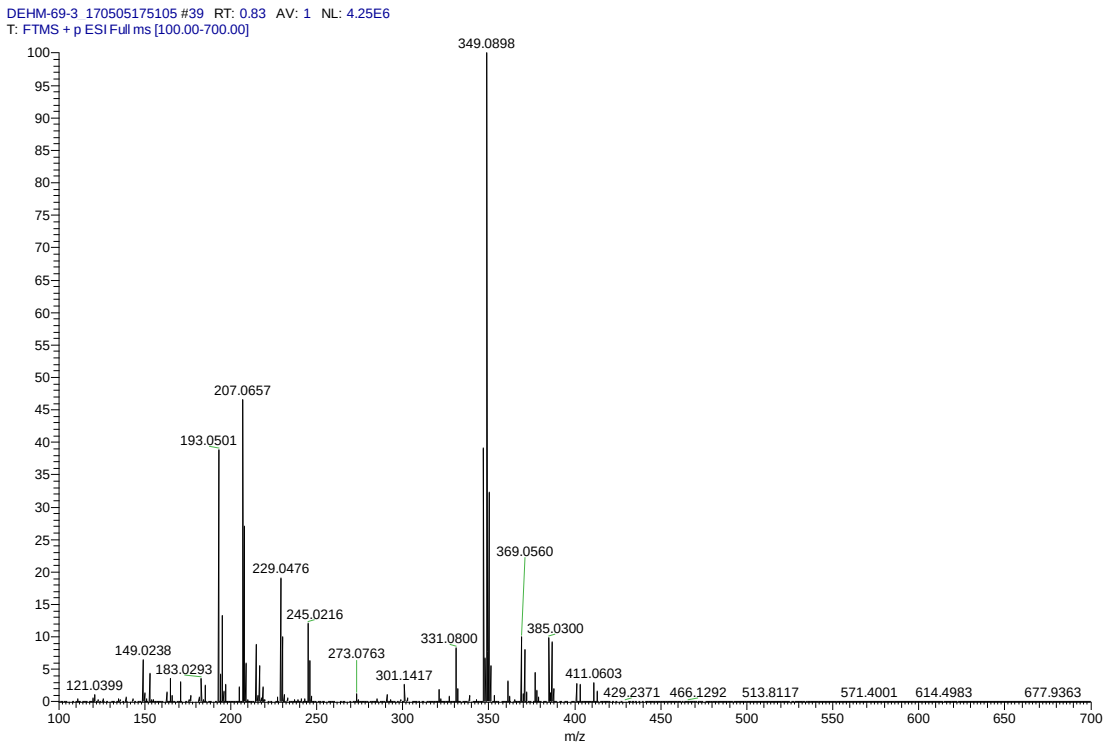

Figure S35. HRESIMS Spectrum of compound **5** in MeOD

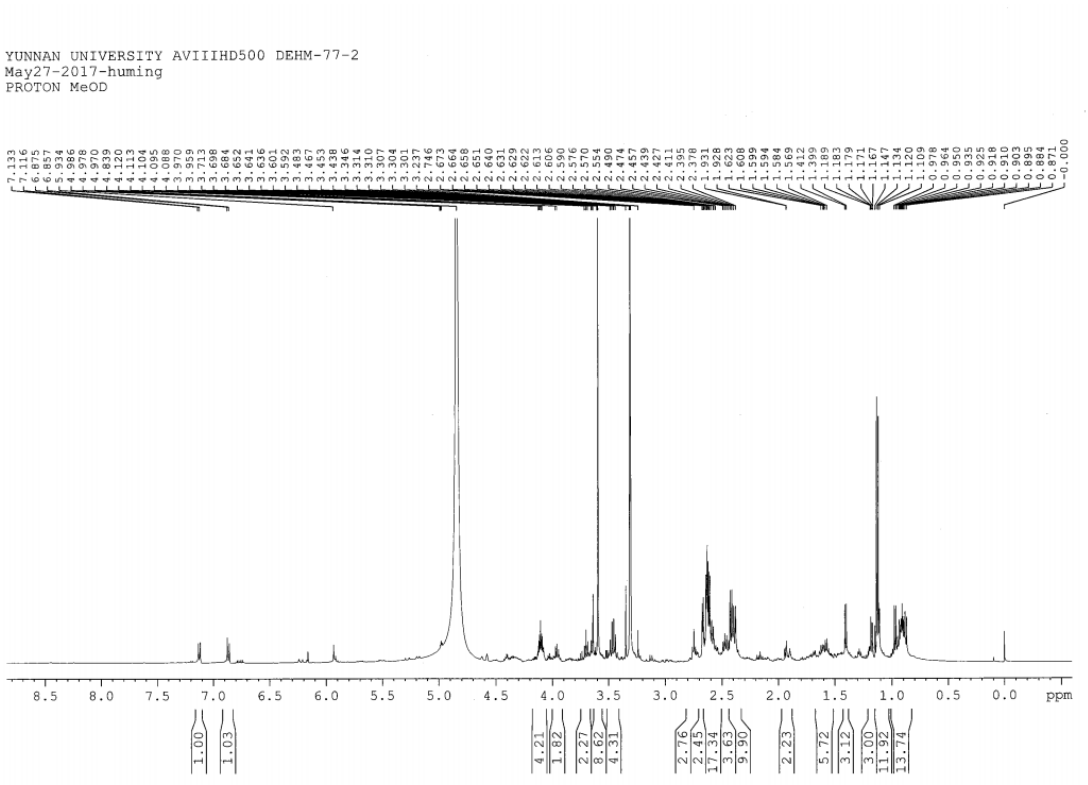

Figure S36. ^{1}H NMR of compound **6**

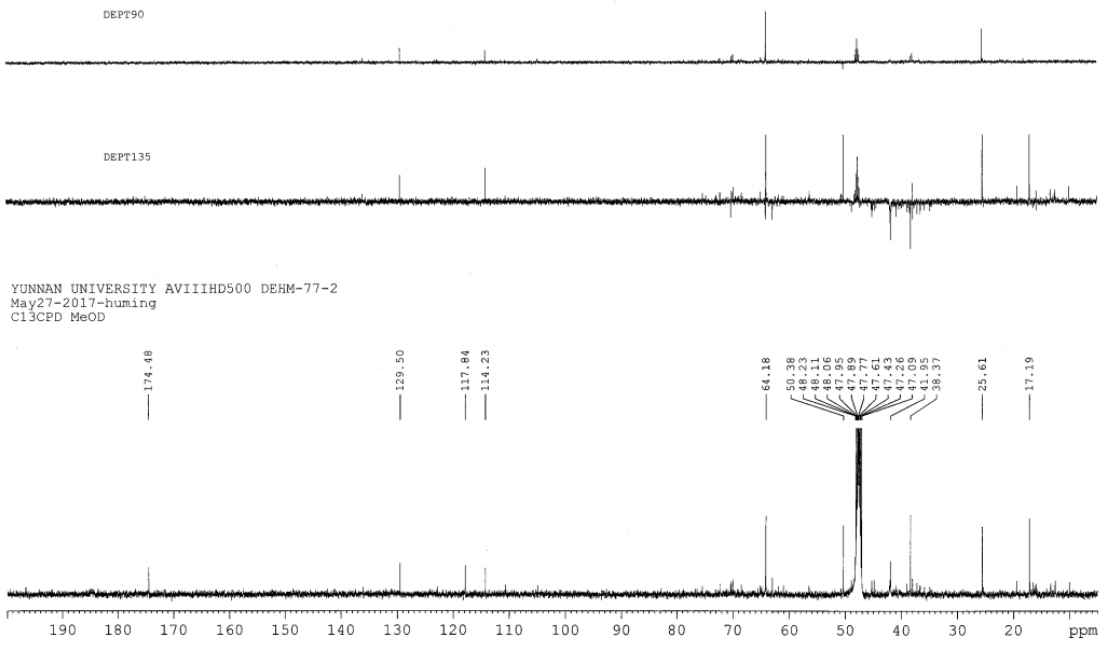

Figure S37. ^{13}C NMR of compound **6**

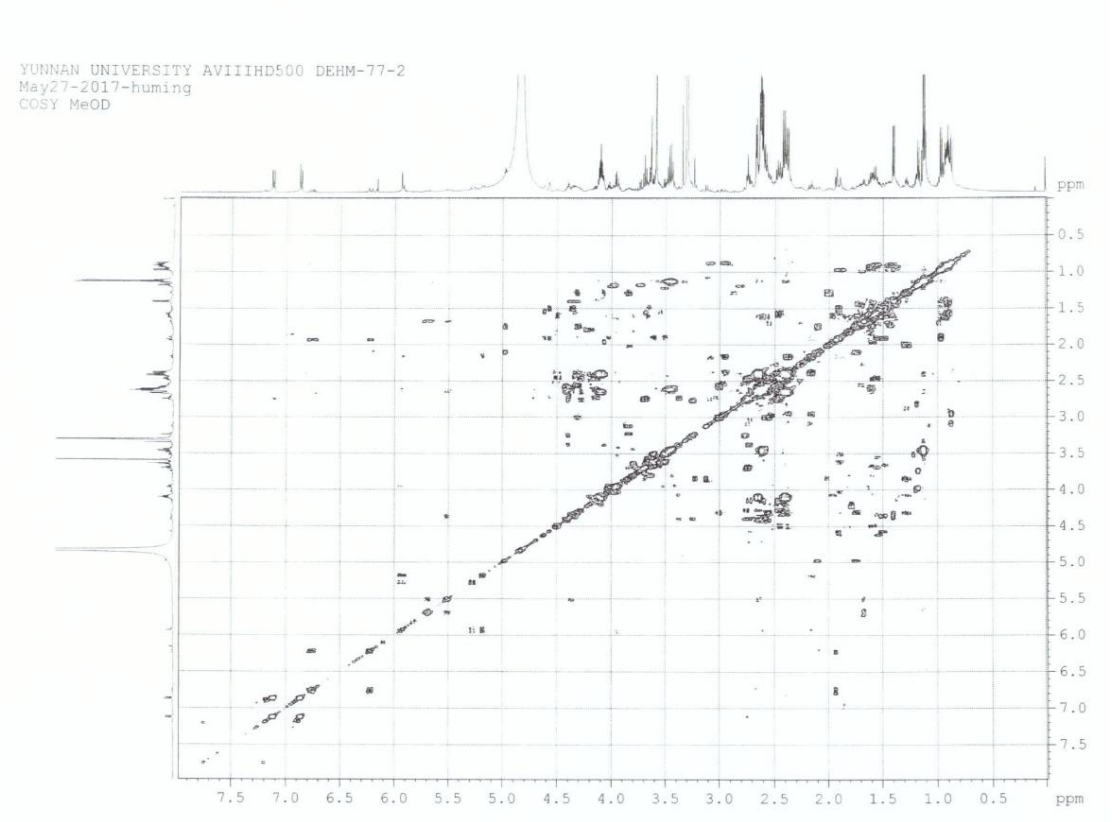

Figure S38. ^{1}H-^{1}H COSY Spectrum of compound **6** in MeOD

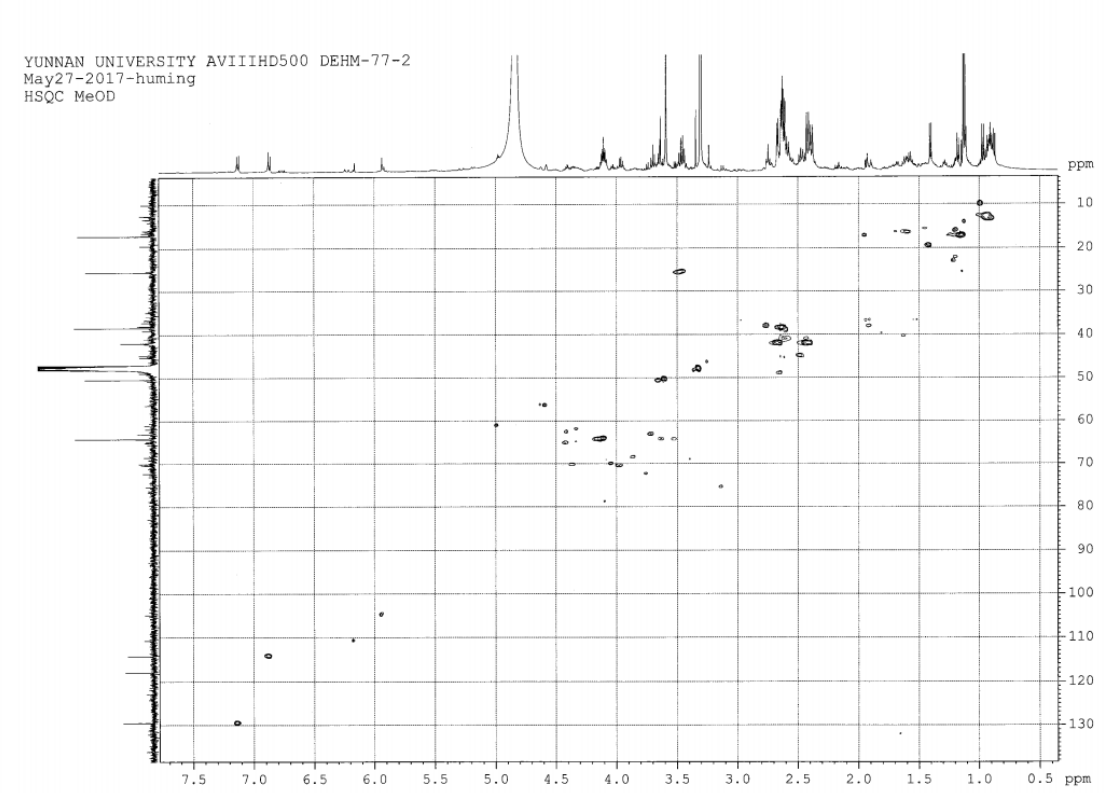

Figure S39. HSQC Spectrum of compound **6** in MeOD

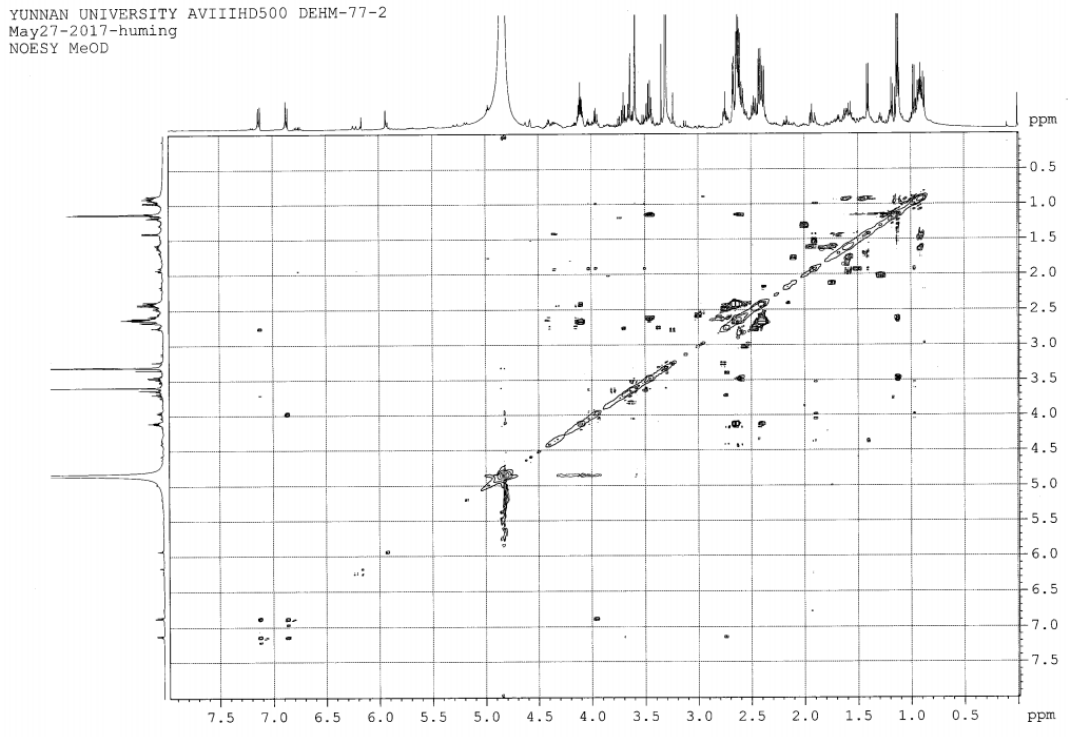

Figure S40. ROESY Spectrum of compound **6** in MeOD

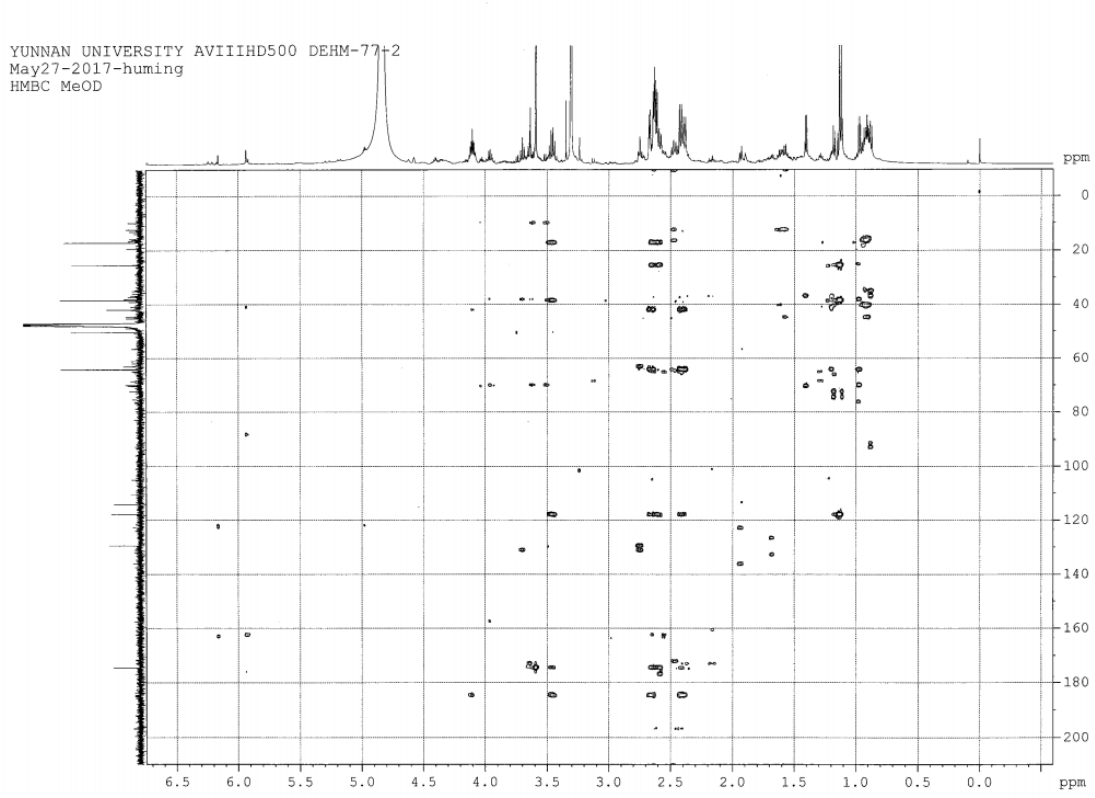

Figure 41. HMBC Spectrum of compound **6** in MeOD

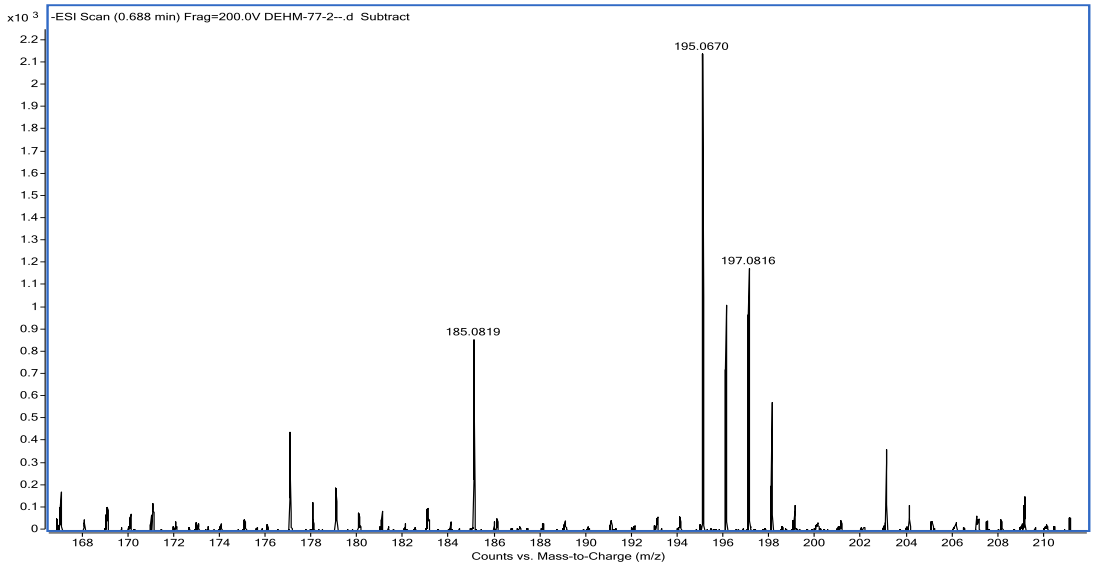

Figure S42. HRESIMS Spectrum of compound **6**

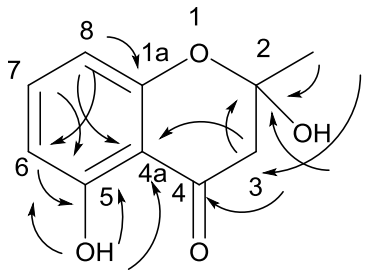

Figure S43. The key HMBC correlations of compound **1**.

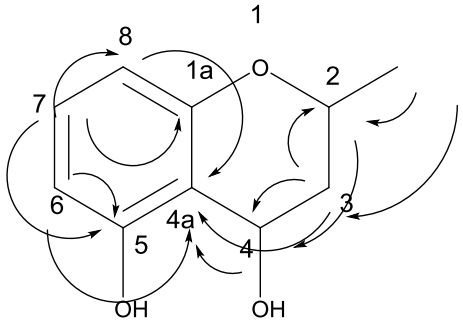

Figure S44. The key HMBC correlations of compound **2.**

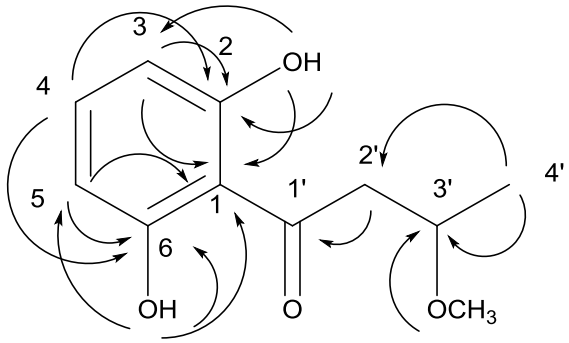

Figure. S45. The key HMBC correlations of compound **3**.

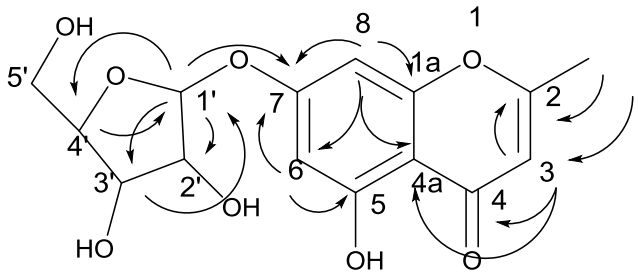

Figure S46. The key HMBC correlations of compound **4**.

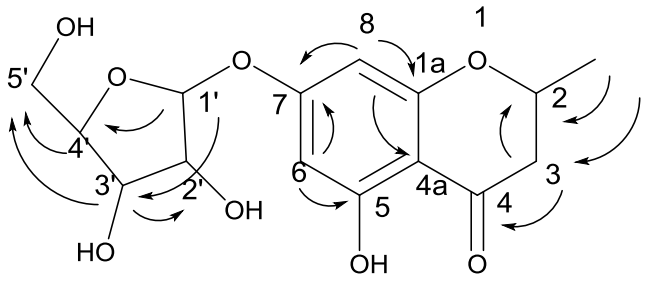

Figure S47. The key HMBC correlations of compound **5**.

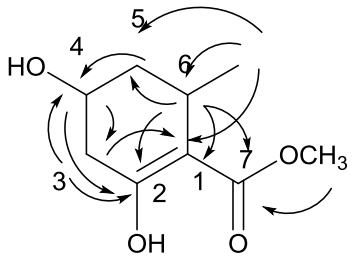

Figure S48. The key HMBC correlations of compound **6**.

Table S1. ^{13}C NMR (100 MHz) and ^{1}H NMR (400 MHz) data of compounds **1**-**3** in $CDCl_3$

Pos.	**1**		**2**		Pos.	**3**	
	δ_H	δ_c	δ_H	δ_c		δ_H	δ_c
1a		158.5		155.5	1		113.3
2		101.0	4.19 (m)	71.1	2		160.6
3	2.93 (d, J=11.2 Hz)	47.4	1.82, 2.33(m)	38.8	3	6.44 (d, J=8.4Hz)	109.3
4		197.4	5.20 (m)	65.4	4	7.25 (t, J=8.4 Hz)	137.1
4a		108.1		111.0	5	6.44 (d, J=8.4Hz)	109.3
5		162.1		156.6	6		160.8
6	6.54 (d, J=8.4 Hz)	110.3	6.40 (d, J=8.0 Hz)	108.3	1′		205.1
7	7.36 (t, J=8.4 Hz)	138.6	7.04 (t, J=8.0 Hz)	129.6	2′	2.68, 3.48 (m)	49.1
8	6.41 (d, J=8.4 Hz)	107.8	6.44 (d, J=8.0 Hz)	108.4	3′	4.08 (m)	78.0
CH_3	1.74 (s)	29.0	1.41 (d, J=6.4 Hz)	21.2	4′	1.35 (d, J=6.0 Hz)	18.8
					OCH_3	3.37 (s)	56.6

Table S2. ^{13}C NMR and ^{1}H NMR data of compounds **4**-**6** in MeOD

Pos.	**4**		**5**		Pos.	**6**	
	δ_H	δ_c	δ_H	δ_c		δ_H	δ_c
1a		159.7		162.8	1		117.8
2		170.2	4.59 (brs)	75.6	2		183.7
3	6.10 (s)	109.5	2.61 (m)	44.3	3	2.43, 2.64 (m)	42.0
4		184.5		198.7	4	4.12 (m)	64.2
4a		106.9		104.6	5	2.64 (m)	38.4
5		163.2		164.7	6	3.45 (m)	25.6
6	6.53 (s)	101.6	6.18 (s)	98.1	7		174.5
7		165.0		166.8	OCH_3	3.59 (s)	50.4
8	6.71 (s)	96.6	6.18 (s)	97.1	CH_3	1.12 (d, J= 5.5 Hz)	17.2
CH_3	2.38 (s)	20.7	1.43 (d, J=6.0 Hz)	21.0			
1′	5.71 (d, J=4.4 Hz)	102.2	5.67 (brs)	101.6			
2′	4.21 (m)	73.8	4.17 (m)	73.5			
3′	4.12 (m)	71.4	4.08 (m)	71.1			
4′	4.12 (m)	88.5	4.08 (m)	88.3			
5′	3.68 (m)	63.4	3.60, 3.67(m)	63.1			